# Geologic Map and Cross Sections of the Embudo Fault Zone in the Southern Taos Valley, Taos County, New Mexico

Paul W. Bauer[1], Keith I. Kelson[2], V.J.S. Grauch[3], Benjamin J. Drenth[3], Peggy S. Johnson[1], Scott B. Aby[4], Brigitte Felix[1]

*[1]New Mexico Bureau of Geology and Mineral Resources, New Mexico Institute of Mining and Technology; [2]U.S. Army Corps of Engineers; [3]U.S. Geological Survey; [4]Muddy Spring Geology, New Mexico.*

Open-File Report 584
November 2016

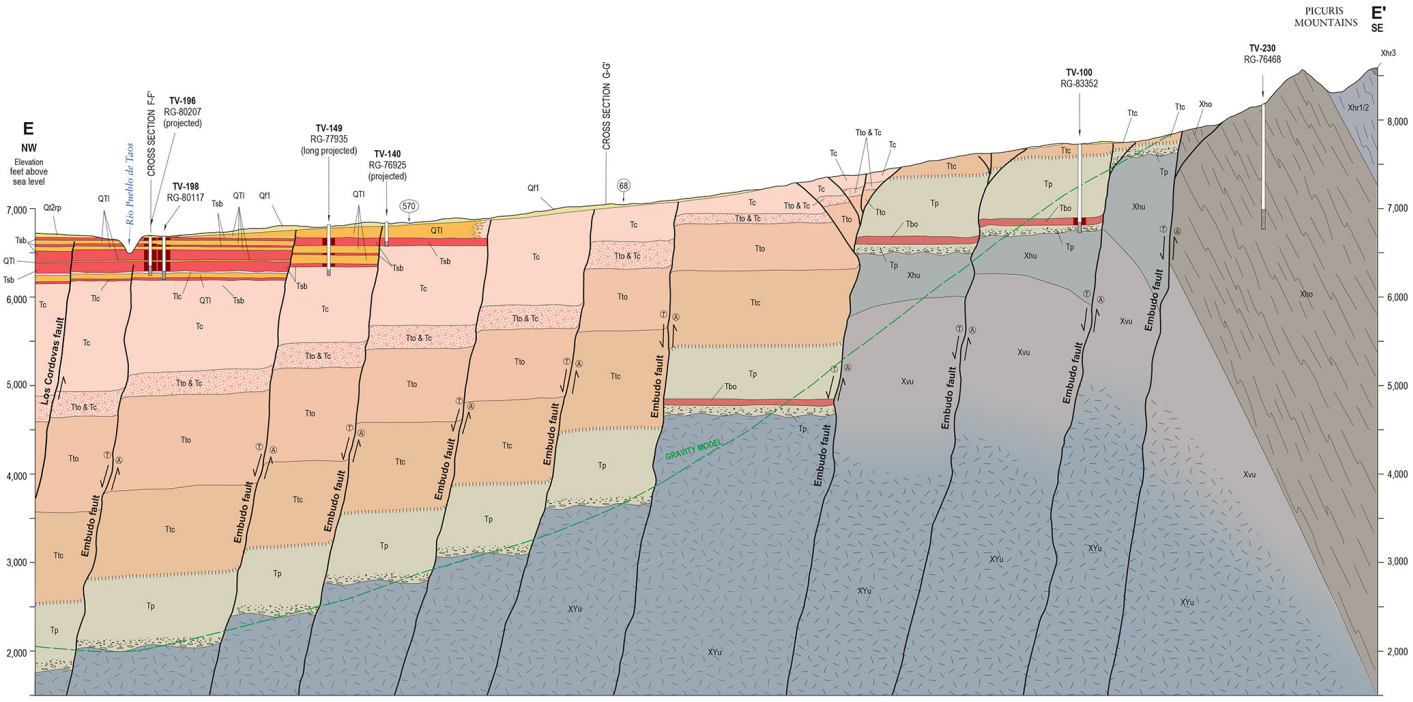

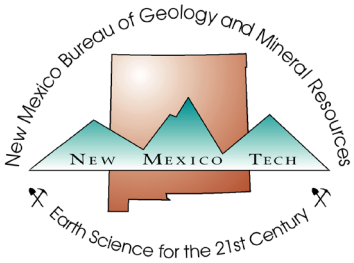


New Mexico Bureau of Geology and Mineral Resources

A division of New Mexico Institute of Mining and Technology

Socorro, NM 87801
(575) 835 5490
Fax (575) 835 6333
geoinfo.nmt.edu

*Suggested Citation:*

Bauer, P.W., Kelson, K.I., Grauch, V.J.S., Drenth, B.J., Johnson, P.S., Aby, S.B., and Felix, B., 2016, Geologic Map and Cross Sections of the Embudo Fault Zone in the Southern Taos Valley, Taos County, New Mexico: New Mexico Bureau of Geology and Mineral Resources Open-File Report 584, 28 p. plus two appendices and two oversized plates.

# Geologic Map and Cross Sections of the Embudo Fault Zone in the Southern Taos Valley, Taos County, New Mexico

Paul W. Bauer[1], Keith I. Kelson[2], V.J.S. Grauch[3], Benjamin J. Drenth[4], Peggy S. Johnson, Scott B. Aby[5], Brigitte Felix[6]

[1] *New Mexico Bureau of Geology and Mineral Resources, New Mexico Institute of Mining and Technology, 801 Leroy Place, Socorro, NM 87801, paul.bauer@nmt.edu*
[2] *U.S. Army Corps of Engineers, South Pacific Division Dam Safety Production Center, 1325 J Street, Sacramento, CA 95814, keith.i.kelson@usace.army.mil*
[3] *U.S. Geological Survey, MS 964, Federal Center, Denver, CO 80225, tien@usgs.gov*
[4] *U.S. Geological Survey, MS 964, Federal Center, Denver, CO 80225, bdrenth@usgs.gov*
[5] *Muddy Spring Geology P.O. Box 488 Dixon, NM 87527, scottandlluvia@gmail.com*
[6] *New Mexico Bureau of Geology and Mineral Resources, New Mexico Institute of Mining and Technology, 801 Leroy Place, Socorro, NM 87801, bfk@nmbg.nmt.edu*

Open-File Report 584
November 2016

AQUIFER MAPPING PROGRAM

New Mexico Bureau of Geology and Mineral Resources

# PROJECT FUNDING

Project funding came from the New Mexico Bureau of Geology and Mineral Resources, U.S. Geological Survey (USGS), Taos County, and the Healy Foundation

# CONTENTS

View west across the Picuris piedmont from just east of Ponce de Leon spring. The orange rocks in the foreground are Proterozoic rocks of the Miranda Granite. Arroyo Miranda runs from left to right in the middle distance, with the homes of the Ponce de Leon neighborhood built on Tertiary rocks of the Picuris Formation. On the left horizon are the Proterozoic rocks of the Picuris Mountains, which grade northward down the Picuris piedmont to the Rio Pueblo de Taos canyon. On the distant skyline to the right are the Proterozoic rocks of the Tusas Mountains. *Photo by Paul Bauer.*

# ABSTRACT

The southern Taos Valley encompasses the physiographic and geologic transition zone between the Picuris Mountains and the San Luis Basin of the Rio Grande rift. The Embudo fault zone is the rift transfer structure that has accommodated the kinematic disparities between the San Luis Basin and the Española Basin during Neogene rift extension. The eastern terminus of the transfer zone coincides with the intersection of four major fault zones (Embudo, Sangre de Cristo, Los Cordovas, and Picuris-Pecos), resulting in an area of extreme geologic and hydrogeologic complexities in both the basin-fill deposits and the bedrock.

Although sections of the Embudo fault zone are locally exposed in the bedrock of the Picuris Mountains and in the late Cenozoic sedimentary units along the top of the Picuris piedmont, the full proportions of the fault zone have remained elusive due to a pervasive cover of Quaternary surficial deposits. We combined insights derived from the latest geologic mapping of the area with deep borehole data and high-resolution aeromagnetic and gravity models to develop a detailed stratigraphic/structural model of the rift basin in the southern Taos Valley area.

The four fault systems in the study area overlap in various ways in time and space. Our geologic model states that the Picuris-Pecos fault system exists in the basement rocks (Picuris formation and older units) of the rift, where it is progressively down dropped and offset to the west by each Embudo fault strand between the Picuris Mountains and the Rio Pueblo de Taos. In this model, the Miranda graben exists in the subsurface as a series of offset basement blocks between the Ponce de Leon neighborhood and the Rio Pueblo de Taos. In the study area, the Embudo faults are pervasive structures between the Picuris Mountains and the Rio Pueblo de Taos, affecting all geologic units that are older than the Quaternary surficial deposits. The Los Cordovas faults are thought to represent the late Tertiary to Quaternary reactivation of the old and deeply buried Picuris-Pecos faults. If so, then the Los Cordovas structures may extend southward under the Picuris piedmont, where they form growth faults as they merge downward into the Picuris-Pecos bedrock faults.

The exceptionally high density of cross-cutting faults in the study area has severely disrupted the stratigraphy of the Picuris formation and the Santa Fe Group. The Picuris formation exists at the surface in the Miranda and Rio Grande del Rancho grabens, and locally along the top of the Picuris piedmont. In the subsurface, it deepens rapidly from the mountain front into the rift basin. In a similar manner, the Tesuque and Chamita Formations are shallowly exposed close to the mountain front, but are down dropped into the basin along the Embudo faults. The Ojo Caliente Sandstone Member of the Tesuque Formation appears to be thickest in the northwestern study area, and thins toward the south and the east. In the study area, the Lama formation thins westward and southward. The Servilleta Basalt is generally thickest to the north and northwest, thins under the Picuris piedmont, and terminates along a major, linear, buried strand of the Embudo fault zone, demonstrating that the Servilleta flows were spatially and temporally related to Embudo fault activity.

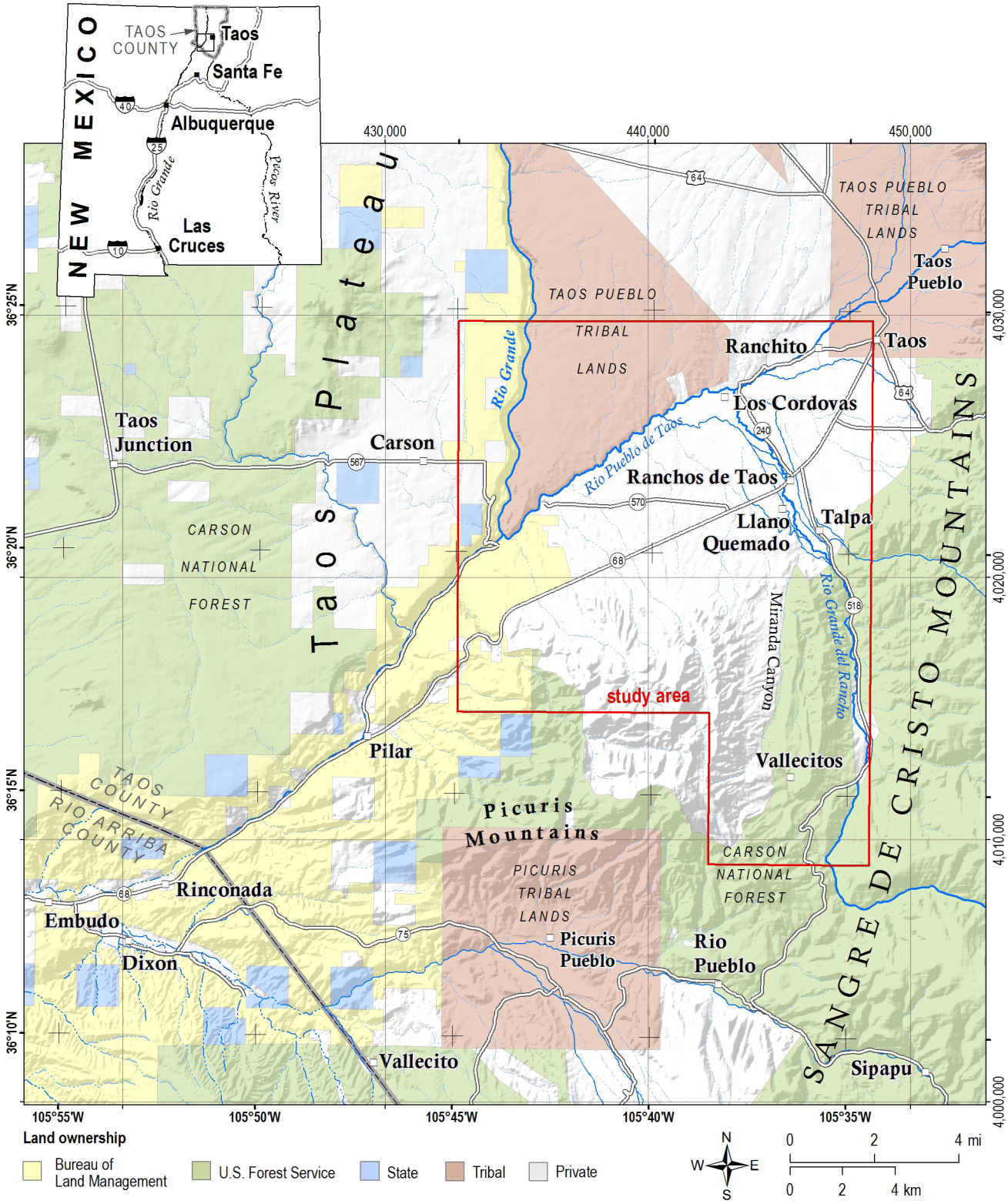


**Figure 1.** Location map, land status, and regional setting of southern Taos Valley. The study area is outlined in red.

# I. INTRODUCTION

## Background

In 2011, the New Mexico Bureau of Geology and Mineral Resources (NMBGMR) entered into an agreement with Taos County, New Mexico, to study the hydrogeology of the southern Taos Valley (Johnson et al., 2016). An essential component of the investigation was to develop a state-of-the-art geologic model of the study area that could be used to develop a geologically based hydrogeologic model of the groundwater and surface water of the area. In order to develop the geologic model, NMBGMR geologist Paul Bauer collaborated with U.S. Geological Survey (USGS) geophysicists Tien Grauch and Ben Drenth, who were using high-resolution aeromagnetic and gravity data to discern the architecture of the San Luis Basin in New Mexico and Colorado. This collaboration turned out to be highly productive, and led to the development of an unprecedented set of geologic cross sections that are firmly rooted in the newest and most robust stratigraphic and geophysical models of the basin. These cross sections reveal an extraordinarily complex network of faulted bedrock and basin-fill deposits in this region of the Rio Grande rift.

## Previous Work

A series of geologic quadrangle maps has been produced by the NMBGMR (http://geoinfo.nmt.edu/publications/maps/geologic/ofgm/home.cfm) including maps of the entire southern Taos Valley study area (Bauer et al., 2016). Regional geologic maps (Miller et al., 1963; Lipman and Mehnert, 1975; Machette and Personius, 1984; Garrabrant, 1993) and thesis maps of generally small areas or specialized subjects (Chapin, 1981; Peterson, 1981; Leininger, 1982; Rehder, 1986; Kelson, 1986; Bauer, 1988) also exist in the study area. A preliminary geologic and hydrogeologic analysis of the southeastern Taos Valley (Bauer et al., 1999) slightly overlaps with the eastern edge of the current study area.

The 2004 New Mexico Geological Society Guidebook (Brister et al., 2004) contains papers on the stratigraphy, structural geology, and geophysics of the Taos Valley area. Several of those papers pertain to the faulting in the study area, including an analysis of the Embudo fault zone (Kelson et al., 2004a) and an evaluation of the rates of extension along the Embudo fault and across the rift (Bauer and Kelson, 2004a). A study of the earthquake potential of the Embudo fault zone (Kelson et al., 1997) included detailed geomorphic mapping and kinematic analysis of faults on the Picuris piedmont from Pilar to Talpa. Drakos et al. (2004a) described the subsurface stratigraphy of the southern San Luis Basin. Other contributors include Grauch and Keller (2004), Bankey et al. (2006), Drenth et al. 2015, Grauch et al. (2015), who provided updated interpretations of regional geophysical studies of the southern San Luis Basin. Grauch et al. (2017) combined the latest geology and geophysics into a geometric and kinematic model of the northeastern Embudo transfer zone.

## Purpose and Scope

The geologic map and cross sections in this report were originally developed to support a hydrogeologic investigation of the southern Taos Valley (Johnson et al., 2016). The principal focus of the southern Taos Valley report was groundwater, whereas, the principal objective of this derivative report was to characterize and interpret the shallow three-dimensional geology of the northeastern Embudo fault zone area in the southeastern San Luis Basin. This report contains a detailed geologic map, 10 geologic cross sections, a discussion on how the cross sections were created, and a list of notable findings.

## Description of the Study Area

The southern Taos Valley study area is situated at the southern end of the San Luis Basin of northern New Mexico and southern Colorado. The Rio Grande occupies a deep canyon along the west

edge of the study area. In New Mexico, the Rio Grande gorge separates the Taos Plateau to the west from the piedmont slopes to the east, which rise gently eastward to join the Taos Range of the Sangre de Cristo Mountains (Fig. 1). The Taos Plateau is a low-relief landscape that is punctuated by broad, high-relief volcanoes.

The highlands in the southern part of the study area are the Picuris Mountains, a westward prong of the Sangre de Cristo Mountains. The Picuris Mountains drain northward across large alluvial fan deposits to the Rio Pueblo de Taos. The area between the mountains and the Rio Pueblo de Taos is referred to as the "Picuris piedmont."

The study area (92 $mi^2$, 238 $km^2$) includes the foothills of the Picuris Mountains, including much of Miranda Canyon and the Picuris piedmont, which extends northward to the Rio Pueblo de Taos, eastward to just past the Rio Grande del Rancho valley, and westward to the Rio Grande gorge (Fig. 1). The area includes the unincorporated traditional communities of Ranchos de Taos, Talpa, Llano Quemado, Los Cordovas, and Ranchito, as well as eight Taos County neighborhood associations.

# II. METHODS

## Geologic Map and Cross Sections

The geologic map created for this study integrates sections of six geologic maps of 7.5-minute quadrangles that were completed under the NMBGMR STATEMAP Program.

The maps are credited as follows:

1. Taos SW quadrangle (Bauer et al., 1997)
2. Ranchos de Taos quadrangle (Bauer et al., 2000)
3. Taos quadrangle (Bauer and Kelson, 2001)
4. Los Cordovas quadrangle (Kelson and Bauer, 2003)
5. Peñasco quadrangle (Bauer et al., 2005)
6. Tres Ritos quadrangle (Aby et al., 2007)

The 1:24,000-scale compilation map (Plate 1) shows the distribution of rock units and unconsolidated, surficial sand and gravel deposits, as well as the locations of known and inferred faults. Some of the geologic units shown in the cross sections are not exposed at the surface in the study area, but are exposed in nearby areas where they have been mapped and analyzed. The physical characteristics of some of these units (such as composition, thickness, texture, and lateral extent) are based on work in these nearby areas. Geologic unit descriptions are included in Appendix 1.

A primary goal of the investigation was to provide a conceptual model of the large-scale geologic structure of the basin beneath the southern Taos Valley. Our approach was to understand the surficial structural geology around the edge of the basin through detailed mapping, and then to infer the subsurface basin structure using that knowledge and all other available data sets, including:

- photographic imagery
- boreholes
- geophysics
- surface structure
- geomorphology
- hydrogeology

We created 10 new geologic cross sections for this study (Plate 2). The locations of the sections were chosen to optimize hydrogeologic understanding, maximize the number of useful deep boreholes that could be incorporated into the section lines, and utilize all available geophysical insights. Appendix 2 contains a list of all the wells that were used on the geologic map (Plate 1) and geologic cross sections (Plate 2). The topographic profiles were generated by ArcGIS software. The cross sections on Plate 2 have no vertical exaggeration in order to accurately depict the stratigraphic and structural relationships.

The geologic units shown in the cross sections originated from three principal data sources:

1. 1:24,000 geologic quadrangle maps;
2. Interpretations from borehole geology and borehole geophysics; and
3. Interpretations from three geophysical data sets (high-resolution aeromagnetic survey, ground-magnetic surveys, and gravity modeling).

The applications of these data sets in creating the geologic map and cross sections are summarized below.

### Aerial photogrammetry and field mapping

As part of delineating bedrock units, faults, and basin-fill sediments, the mappers analyzed multiple sets of photographic imagery, all of which have a high degree of clarity and provide good information on surficial deposits and fault-related features. Because of their good coverage and high quality, the air-photo analysis primarily utilized 1:15,840-scale color images taken for the U.S. Forest Service from 1973 to 1975. Following our analysis of aerial photography, we conducted detailed mapping of geologic units and geomorphic features at a scale of 1:12,000 (1:6000 in the Talpa area). Our mapping delineated Quaternary deposits and surfaces, and Quaternary faults, fault scarps, and lineaments. Analysis of faults in all units (Proterozoic to Quaternary) included evaluations of fault geometries and kinematic data. Along bedrock faults, fault striations (slickenlines) were combined with kinematic indicators such as offset piercing lines

or planes, and calcite steps to infer slip directions. Because of limited fault exposures in Quaternary deposits, we inferred slip directions based on fault scarp geometry, the geologic map pattern of fault strands, and deflected drainages.

### Boreholes

The geologic and geophysical data attached to the drill holes in the study area ranged from wells with no data, to wells with extensive analyses of lithologic cuttings, different types of borehole geophysics, and a variety of aquifer and water-quality tests. Domestic well records in the study area are marginally useful for defining the subsurface stratigraphy, as most well drillers do not record the detailed characteristics of well cuttings. In contrast, geologic logs created by on-site geologists who examined well cuttings were generally very helpful for defining the subsurface stratigraphy.

### Geophysics

A number of existing and new USGS geophysical studies in the area were incorporated into this investigation. Although each of these geophysical techniques can be used alone to provide useful constraints on the subsurface geology, their value is greatest when they are interpreted collectively, yielding immensely valuable, detailed information on the subsurface geology. Each of the geophysical studies used in the current study are summarized below.

1. Existing high-resolution aeromagnetic data: In 2003, the USGS began conducting high-resolution aeromagnetic surveys in the San Luis Basin (Bankey et al., 2004, 2005, 2006, 2007). Data from these surveys were digitally merged and processed for the study area to show both buried faults and volcanic rocks (Grauch et al., 2004, 2017). This method can be effective at delineating buried, large-scale, horizontal and vertical variations in rock type.
2. New ground-magnetic surveys: In 2011, the USGS ran several, ground-based magnetic traverses on the Picuris piedmont (Grauch et al., 2017). This method can precisely locate buried faults and other features that juxtapose materials with different magnetic properties.
3. Gravity surveys and regional gravity model: Gravity data have been collected in the area as part of this and previous studies (Drenth et al., 2011). The new data were merged with existing public data (http://research.utep.edu/Default.aspx?alias=research.utep.edu/paces) then used to develop a regional, three-dimensional model of the basin (Drenth et al., 2015). The primary goal is to improve our understanding of the thickness of the basin-fill materials and the geometry of the rift basin. The gravity method is especially useful for estimating the general depth to basement rocks and for locating large-offset basement faults.

### Development of the cross sections

The following list describes the general steps that were taken to draw each of the geologic cross sections.

1. Geologic contacts were derived from the geologic map. The surface geology was taken from the geologic map and placed on the topographic profile. Geologic contacts that are buried by thin surficial deposits were estimated. Some of the thinnest Quaternary surficial deposits are not shown on the cross sections.
2. The gravity model was used to define an elevation curve that represents the depth of the contact between basin fill and basement rocks in each cross section. This depth-to-basement curve depicts a highly smoothed contact between basin-fill sediments and bedrock. In the model, both Paleozoic sedimentary rocks and Proterozoic crystalline rocks were considered to be basement.
3. Geologic information derived from wells and boreholes was added to the cross sections. Expertly studied wells can help control the regional thicknesses and depths of key stratigraphic formations, including some of the basin-fill units such as the informal Lama formation and thick clay horizons. Most of the basin-fill stratigraphy (Tesuque Formation (Tt), Chamita Formation (Tc), and Lama formation (QTl)) consists of poorly sorted, clay-to-boulder sized, alluvial material that was eroded from the nearby Sangre de Cristo Mountains. Unless the compositions and proportions of rock clasts and the color of the sediment are well described, it is not possible to tell them apart in drill holes. Although the depictions of these units on the cross sections were based principally on borehole data, local stratigraphic relationships, and an understanding of the sedimentary systems and geologic processes of the area, it is possible that the thicknesses of

the various basin-fill units are not accurately represented. For example, in many areas where there is no Servilleta Basalt in the subsurface, it is not possible to confidently place the contact between the Chamita Formation (Tc) and the Lama formation (QTl).

4. Mapped and inferred faults were drawn onto the cross sections. For the purposes of this study, the dips of the inferred Embudo faults were estimated to be between 70o and 80o northward, unless evidence existed for some other orientation. In all cases, the geometries of the normal faults drawn in the cross sections are intentionally simplified as single inclined planes, when in fact all of the mapped normal faults in this area have much more complex geometries. They are typically curved, segmented, branched, and composed of multiple overlapping fault planes.
5. Geophyiscs: Additional information gleaned from the geophysics was added to the cross section, such as evidence for deeply buried volcanic rocks.
6. Conceptual models of volcanic and sedimentary processes were incorporated into the cross sections. For example, in the study area, Servilleta Basalt lavas flowed south and southeast, and therefore would be expected to thin across Embudo fault scarps on the Picuris piedmont, and interact in complex ways with north- and northwest-prograding alluvial fans from the Picuris and Sangre de Cristo Mountains.
7. Hydrology: In the Taos County region, the location and characteristics of springs are strongly influenced by the geology (Bauer et al., 2007). Specifically, springs tend to occur where contrasts in the hydraulic properties of the rocks exist. Such contrasts can be created by faults, original variations in rock properties, and post-depositional effects such as cementation.
8. Formation contacts were drawn onto the cross sections. Due to a lack of stratigraphic markers in the southern Taos Valley, the dips of the geologic units are generally unknown. Therefore, unless evidence exists for depicting local dips, contacts were drawn as sub-horizontal. In most of the study area, thicknesses of buried basin-fill units are poorly constrained, and so the cross sections typically show approximate formation thicknesses.
9. The cross sections were checked against geophysical models. After each cross section was drawn, it was evaluated against the aeromagnetic and gravity data by construction of a corresponding geophysical model. In areas where the geophysical model was robust, we were able to fine tune the geologic model. For example, the aeromagnetic model might suggest that a volcanic layer shown in a cross section should be thicker or thinner, or that a fault must juxtapose materials with more extreme variations in magnetic properties. This iterative process between geologist and geophysicist was a powerful tool for developing the geologic models.

### Depiction of faults in the cross sections

The fault structures depicted in the cross sections were established from three data sources:

1. Mapped faults from the geologic map. The geologic map (Plate 1) shows a large number of mapped faults, including: (1) segmented oblique-slip fault splays of the Embudo fault zone along the north flank of the Picuris Mountains; (2) normal faults of the Sangre de Cristo fault zone in the northeastern study area; (3) intrabasinal normal faults of the Los Cordovas fault zone; and (4) bedrock strike-slip faults of the Picuris-Pecos fault system. These faults are displayed with a high degree of certainty and are referred to as "mapped faults."
1. Faults inferred from the magnetic and gravity surveys. Modern geophysical techniques using high-resolution magnetic data and gravity data are capable of identifying buried faults in Rio Grande rift basins, such as in the southern Taos Valley (Grauch et al., 2015, 2017; Drenth et al., 2015). These faults are displayed with a moderate to high degree of certainty and referred to as "geophysical faults." In our study area, there is good correspondence between the mapped faults and the geophysically defined faults, which elevates our confidence in the delineation of buried faults by such geophysical methods. See Grauch et al. (2017) for a comprehensive discussion.
3. A conceptual model of the geometry and kinematics of the northern Rio Grande rift. As the depth-to-basement curve drops into the basin, numerous buried faults must exist in order to deepen the basement. Their exact locations are shown with a low degree of certainty, and they are referred to as "inferred faults."

# III. GEOLOGY

## Regional Geology

### Rio Grande rift

The Rio Grande rift in northern New Mexico is composed of a series of north-trending, elongate topographic and structural basins, including the San Luis and Española Basins (Fig. 2). The basins are broad half grabens that are tilted to either the east (San Luis Basin) or west (Española Basin), and typically have a relatively active, north-striking fault system along one border as well as numerous, minor-displacement faults within the basin. Current tectonic models and geologic maps show that the basins of the northern Rio Grande rift are separated by northeast-trending fault zones that accommodate the differential sense of basin tilting (Chapin and Cather, 1994).

The 150-mile-long San Luis Basin is bordered by the Sangre de Cristo Mountains on the east, the Tusas and San Juan Mountains on the west, and the Picuris Mountains to the south. The San Luis Basin contains a deep, narrow, structural trough, known as the Taos graben in New Mexico, along the eastern edge of the basin (Bauer and Kelson, 2004b). The western edge of the graben (the Gorge fault) lies beneath the Rio Grande (Cordell and Keller, 1984; Bauer and Kelson, 2004b), resulting in a graben that is less than half the width of the topographic valley. The structural bench west of the Taos graben rises gently to the Tusas Mountains, and is cut by numerous small-displacement normal faults. The southwestern part of the basin is a physiographically and geologically unique terrain known as the Taos Plateau. The plateau is composed of Pliocene volcanoes and lava flows that have only been mildly deformed by rift processes.

The Sangre de Cristo and Embudo fault zones form the eastern and southern boundaries of the basin (Fig. 2). The Sangre de Cristo fault is a north-striking, west-dipping normal fault system that accommodates asymmetric subsidence of the basin. The Sangre de Cristo fault exhibits geomorphic evidence for multiple surface-rupturing events in the late Quaternary (Machette and Personius, 1984; Menges, 1990; Kelson et al., 2004b). The Embudo fault strikes northeast-southwest, and can be interpreted as a transfer fault or accommodation zone (Faulds and Varga, 1998; Kelson et al., 2004a; Bauer and Kelson, 2004b) that allows differential subsidence between the San Luis Basin to the northeast and the Española Basin to the southwest. Detailed field mapping and geomorphic investigations document late Quaternary and possibly Holocene surface rupture along the northeastern Embudo fault (Kelson et al., 1996, 1997, 2004a).

Unlike the rift basins to the south, the San Luis Basin is relatively undissected. That is, the sedimentary material that fills the basin has not yet been extensively eroded and exposed by the action of rivers and streams. Instead, the Rio Grande and its major eastern tributaries have cut several deep, narrow canyons through the volcanic rocks that cap most of the area. The river canyons provide the only good exposures of the basin-fill rocks in the basin. The Rio Grande gorge contains good exposures of Tertiary volcanic rocks, as well as the interlayered sands and gravels that represent westward-prograding alluvial fans of the Taos Range (Peterson, 1981; Dungan et al., 1984).

### Taos Plateau volcanic field

The Pliocene to Pleistocene Taos Plateau volcanic field is the largest and compositionally most diverse volcanic field of the Rio Grande rift. Nearly all of the isolated, rounded mountains scattered across the Taos Plateau are extinct volcanoes that erupted between about 6 and 1 million years ago (Lipman and Mehnert, 1979; Appelt, 1998). At least 35 discrete volcanic vents have been identified on the plateau (Dungan et al., 1984; Appelt, 1998).

The volcanoes of the Taos Plateau occur in a variety of sizes and shapes. Shield volcanoes (such as the vents of La Segita Peaks) are shallow-sloped and constructed of successive lava flows. Lava domes (such as San Antonio Mountain, Ute Mountain, Cerro Chiflo, No Agua Peaks, Cerro del Aire, Cerro de la Olla, and Cerro Montoso) are large, steep-sided volcanoes that were formed from numerous localized eruptions. Flood or plateau basalts (such as the Servilleta Basalt) are fluid lavas that

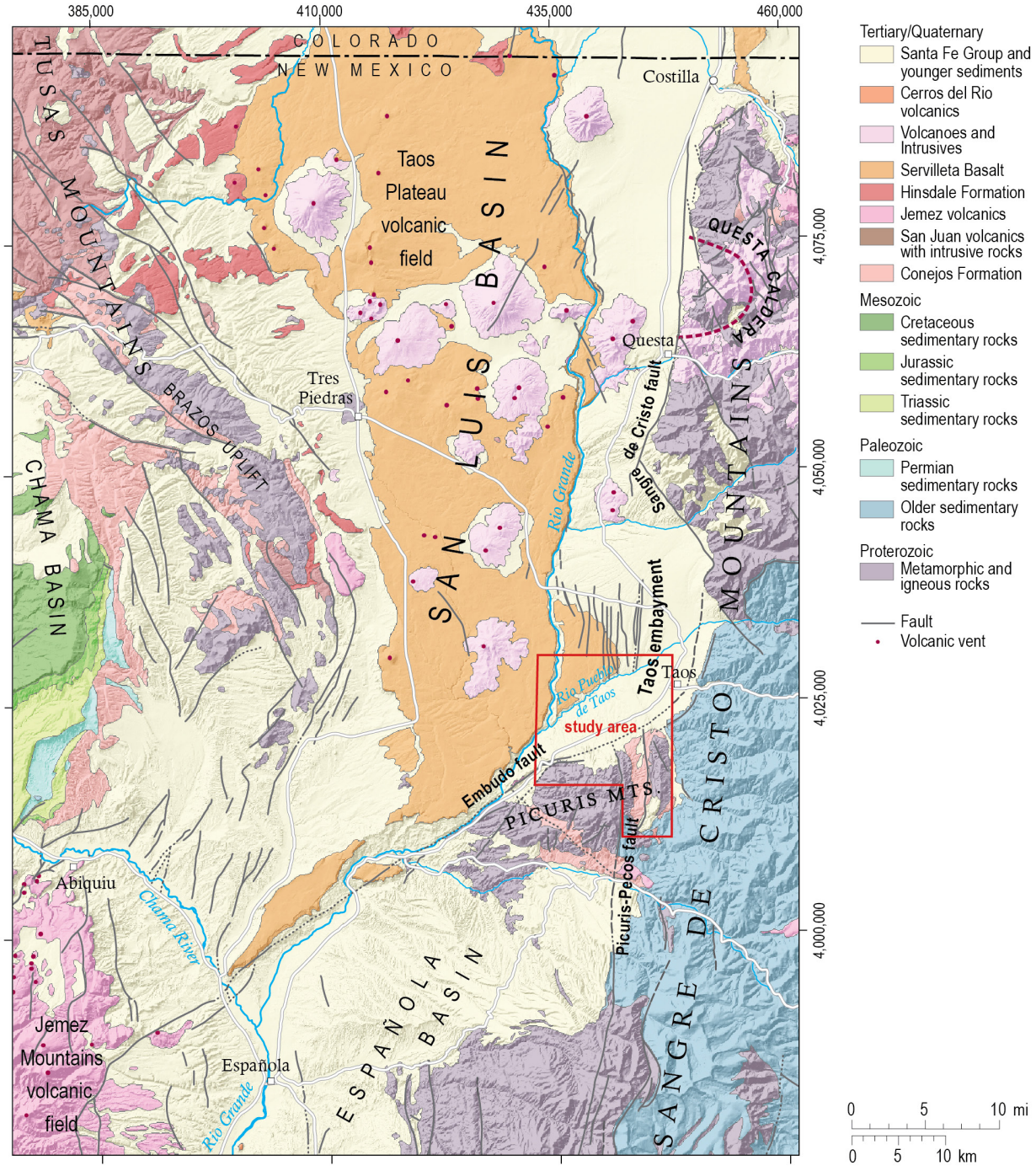


**Figure 2.** Regional geologic map of the southern San Luis Basin of the Rio Grande Rift, with the study area outlined in red. The study area spans the boundary between the San Luis Basin and the Picuris Mountains, and overlaps the structurally complex zone where the older Picuris-Pecos fault system is truncated by Neogene-age, rift bounding faults of the Embudo fault zone just southwest of Taos. In the eastern study area, the northeast-striking Embudo fault zone transitions to the north-striking Sangre de Cristo fault zone. Map is modified from Read et al. (2004).

erupted out of low-relief vents, and flowed many miles before solidifying.

The volcanoes that flank the Rio Grande gorge span a wide variety of compositions (Lipman and Mehnert, 1979). Although most are mafic to intermediate in composition (basalts, andesites, dacites), rhyolites are not uncommon. Ute Mountain, San Antonio Mountain, Guadalupe Mountain, Cerro de la Olla, Cerro Chiflo, Cerro Montoso, and Cerro de los Taoses are andesite or dacite volcanoes that erupted from approximately 3 to 5 million years ago. The principal rhyolite volcano, No Agua Peaks, is about 4 million years old.

The only rocks of the Taos Plateau volcanic field exposed in the study area are Servilleta Basalt flows that exist at the surface, and in the subsurface, in the northern half of the study area.

### Rio Grande gorge

Upon exiting the San Juan Mountains, the Rio Grande turns southward, transects the San Luis Basin, and flows south through successive rift basins toward the Gulf of Mexico. The river follows the topographically lowest part of the rift, carving several spectacular canyons along the way. Beginning in southern Colorado, the Rio Grande has cut a steep-sided basalt canyon known as the Rio Grande gorge. The gorge deepens southward to 850 feet at the Wild Rivers Recreation Area near Questa, and then gradually shallows as the Rio Grande flows through the southern San Luis Basin and into the Española Basin. Several east-side tributaries have cut deep canyons to the Rio Grande, including the Rio Pueblo de Taos, the Rio Hondo, and the Red River.

### Picuris Mountains and Sangre de Cristo Mountains

The southern Rocky Mountains of northern New Mexico have experienced a complex geologic history that spans 1.7 billion years, including multiple mountain-building events. The rocks of the Taos area contain evidence of all of these events. The Taos area straddles the boundary between Paleoproterozoic and Paleozoic basement rocks of the southern Sangre de Cristo Mountains and Paleoproterozoic to Mesoproterozoic and Paleozoic basement rocks of the Picuris Mountains (Fig. 3). The Proterozoic rocks of the northern Picuris Mountains, which underlie much of the watershed in our study area, consist predominantly of quartzite, schist, and slate. The Sangre de Cristo Mountains along the southeastern edge of the study area, including the headwaters of the Rio Grande del Rancho, consist principally of Paleozoic shale, sandstone, limestone, and conglomerate. The transitional zone between the two mountain ranges, including the Rio Grande del Rancho and Miranda canyons, consists of Proterozoic granite, Paleozoic sedimentary rocks, and Tertiary volcaniclastic sedimentary rocks.

## Geologic Units

The following units are exposed in the study area:

1. Quaternary surficial deposits;
2. Pliocene Servilleta Basalt;
3. Tertiary sedimentary units of the Santa Fe Group;
4. Middle Tertiary sedimentary rocks of the Picuris formation;
5. Paleozoic sedimentary rocks; and
6. Proterozoic crystalline rocks.

These units are shown on the detailed geologic map (Plate 1), a generalized geologic map and stratigraphic chart (Figs. 3, 4), and on a series of geologic cross sections (Plate 2). Detailed descriptions of all geologic units found in the study area are presented in Appendix 1.

### Surficial deposits

Surficial deposits in the study area provide a means of discerning the locations of faults that have been active in the Quaternary, and to estimate the senses and relative amounts of Quaternary movements (Bauer and Kelson, 2004b). The area contains a variety of coalescent alluvial-fan, stream-channel, and terrace deposits that range in age from late Pliocene(?) to Holocene. In the central part of the study area, alluvial fans derived from the Picuris Mountains interfinger with alluvial terrace deposits along the Rio Grande del Rancho north of Talpa (Plate 1). An ash layer in the oldest alluvial fan on the Picuris piedmont was dated at 1.27 ± 0.02 Ma (Bauer et al., 1997).

Along the major streams, near-surface Quaternary units consist of coarse-grained fluvial sediments deposited by the major streams, and coarse- to fine-grained alluvial-fan sediments derived from smaller, mountain-front drainages. The area contains fluvial and alluvial-fan deposits that range in age from early to middle(?) Pleistocene to Holocene. Fluvial sediments exist along the Rio Grande del Rancho,

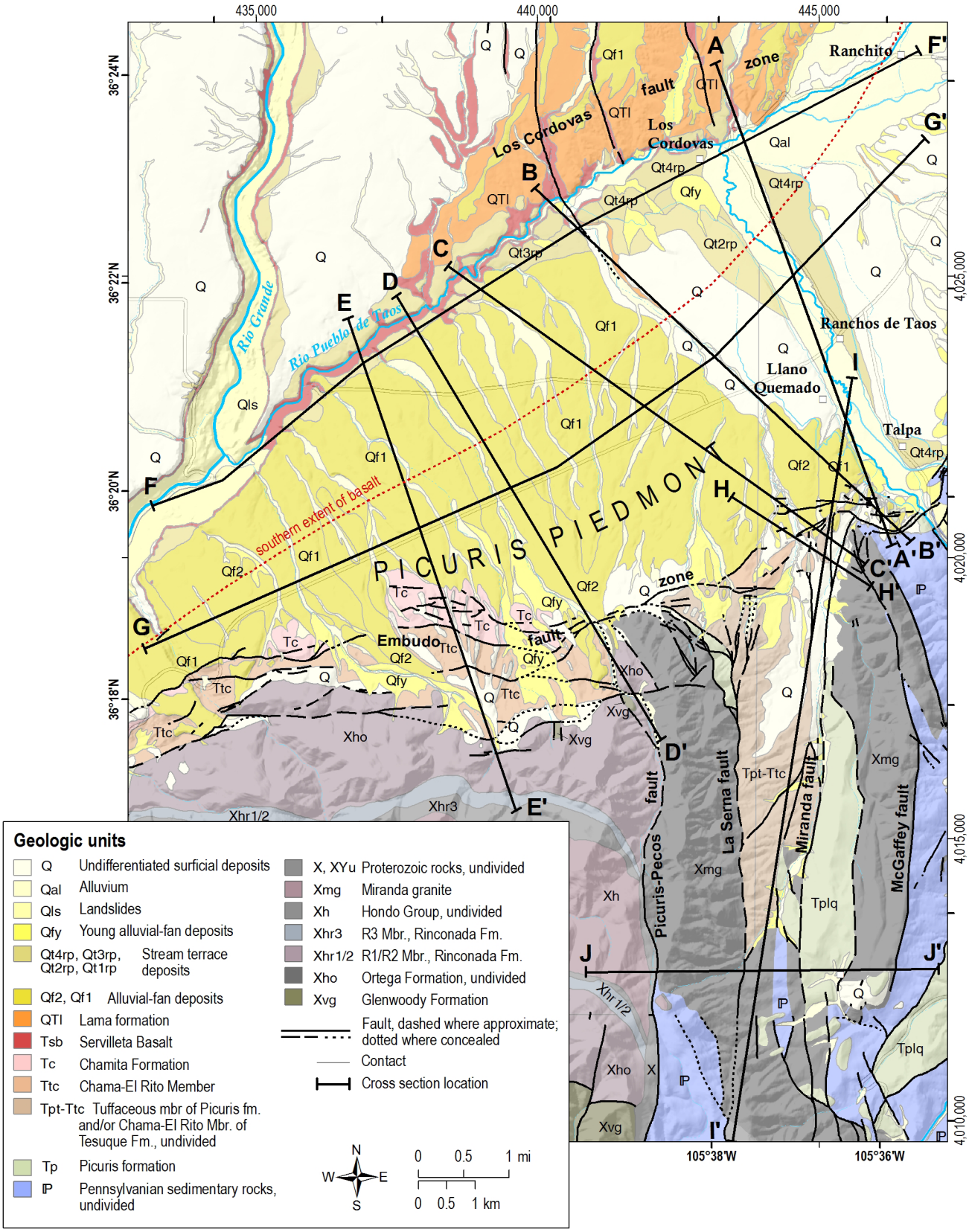


**Figure 3.** Generalized geologic map of the study area, showing cross section lines. This geologic map is simplified from six 7.5-minute quadrangle maps: Los Cordovas quadrangle (Kelson and Bauer, 2003), Carson quadrangle (Kelson et al., 1998), Taos SW quadrangle (Bauer et al., 1997), Taos quadrangle (Bauer and Kelson, 2001), Penasco quadrangle (Bauer et al., 2005), and Tres Ritos quadrangle (Aby et al., 2007). See Appendix 1 for detailed geologic unit descriptions. See Plate 1 for the detailed geologic map. The "southern extent of basalt" line represents the approximate southernmost subsurface occurrence of appreciable thickness of Servilleta Basalt.

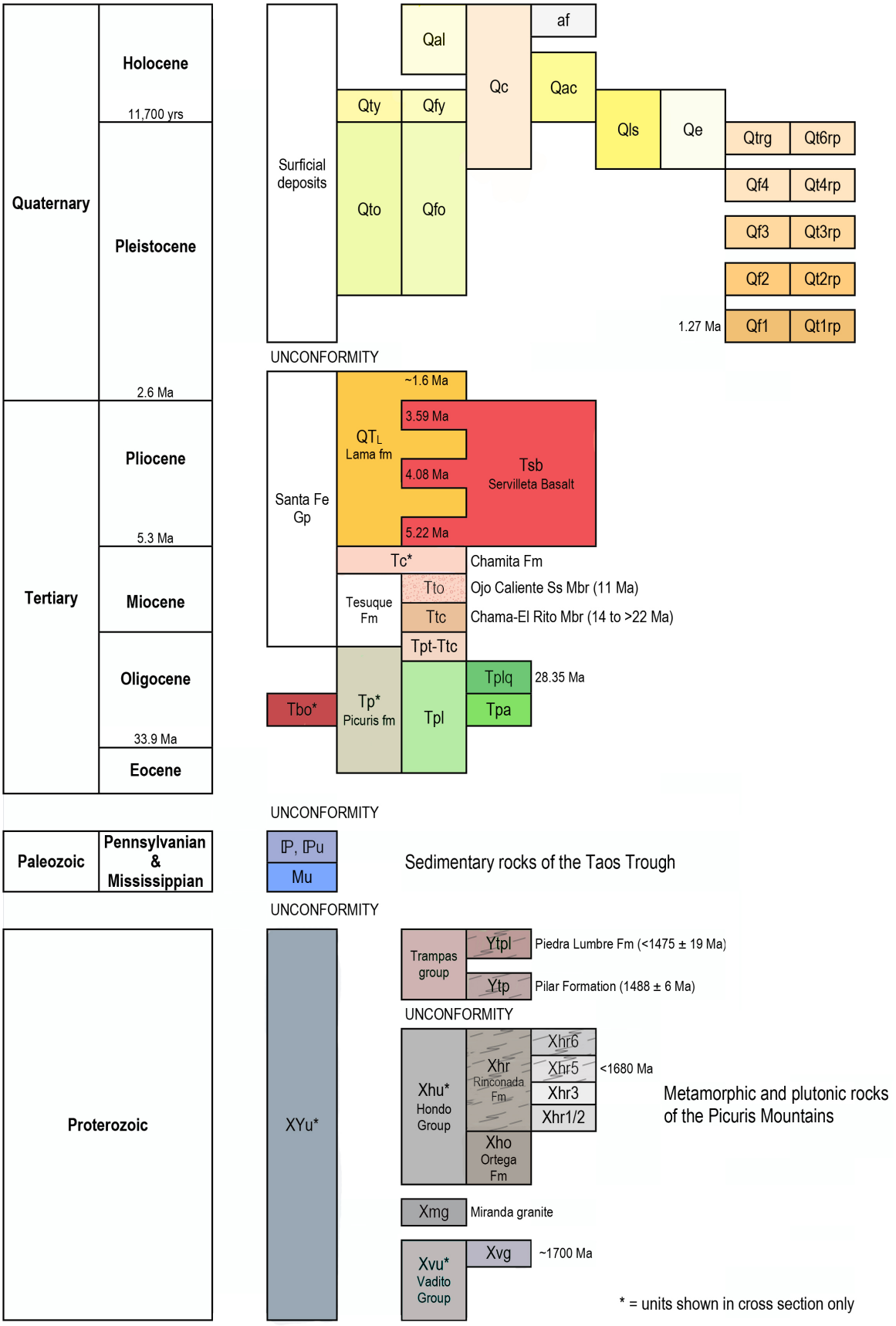


**Figure 4.** Stratigraphic chart of the southern Taos Valley study area, with approximate age on the vertical axis. The chart contains the units found on both the geologic map (Plate 1) and the cross sections (Plate 2).

Rio Chiquito, Rio Pueblo de Taos, and Rio Fernando valleys. These poorly sorted sands and gravel contain subrounded clasts of quartzite, slate, sandstone, schist, and granite, and are laterally continuous in a down-valley direction (Kelson, 1986). Soils developed on these deposits associated with older, higher stream terraces contain well-developed (stage III to IV) calcic horizons. Younger terraces are associated with lesser amounts of soil development (Kelson, 1986).

Alluvial-fan deposits in the eastern part of the study area are derived mostly from smaller mountain-front drainages developed in Pennsylvanian sandstone and shale. In general, these deposits are coarse-grained sands and gravels near the mountain front, and are finer-grained with distance to the north or west (Bauer and Kelson, 2004b). The alluvial-fan deposits likely are laterally discontinuous and moderately heterogeneous. Older fan deposits are associated with well-developed soils (stage III to IV calcic soils), whereas younger deposits contain moderately developed soils (stage I to II calcic horizons) or lesser-developed soils.

### Servilleta Basalt

A single type of volcanic rock volumetrically dominates the Taos Plateau, the olivine tholeiite flood basalts of the Servilleta Basalt. The Rio Grande and Rio Pueblo de Taos gorge walls chiefly consist of thin, near-horizontal layers of this dark gray, pahoehoe, vesicular lava. The basalts were erupted from low-relief shield volcanoes north of the study area, traveling as thin sheets for tens of miles before solidifying. Over 600 feet of basalt were locally stacked up between about 5 and 3 million years ago. These rocks can be seen from any location along the Rio Grande gorge, and in the northwestern part of the study area.

Servilleta Basalt ranges in thickness across the Taos Plateau. Lava flows taper down to zero where they onlap preexisting volcanoes and other highlands. Basalts thin into the study area, and feather out to zero near NM-68. The southern extent of an appreciable thickness of Servilleta Basalt, as inferred from aeromagnetic interpretation, is labeled in Figure 3 and Plate 1 as the "southern extent of basalt" line. The variable thickness and monolithic nature of the basalt flows make them poor stratigraphic markers that cannot be convincingly correlated in the subsurface using well data alone. These fluid lavas clearly flowed around topographic obstructions, and appear to thicken and thin along paleo-fault scarps in the study area.

### Santa Fe Group basin fill

Borehole data in the San Luis Basin indicate that relatively thin Quaternary deposits are underlain by thick Tertiary sedimentary deposits that are dominated by sand and gravel, with lesser amounts of silt and clay. Although some of the Tertiary sediment that fills the rift basin was deposited by the Rio Grande, much of the clay, silt, sand, gravel, and cobbles were eroded from the nearby mountains during the past 25 million years. The San Luis Basin is surrounded by large alluvial fans (and related deposits) that have slowly advanced from the mountains into the basin. In the Rio Grande rift, these principally Neogene deposits are called the Santa Fe Group. Over much of the basin, we can only see the youngest basin fill at the surface. However, glimpses of Santa Fe Group sediments exist along the upper Picuris piedmont, and in the Rio Grande gorge just to the west of the study area. From youngest to oldest, the principal subdivisions of the Santa Fe Group in the study area are the Lama formation, the Chamita Formation, and the Tesuque Formation.

Between the Picuris piedmont and Arroyo Hondo, the Servilleta Basalt is interlayered with, and overlain by, sand and gravel deposits of the Lama formation (Bauer et al., 1997) that likely are the distal parts of alluvial fans shed from the Sangre de Cristo Mountains, and/or derived from the ancestral Rio Grande (Kelson, 1986). These highly oxidized and weathered sediments are probably early to middle Pleistocene in age, and appear to have been extensively saturated by a high water table throughout much of the eastern Taos Plateau. The Lama formation was deposited prior to the development of the Rio Grande gorge (Wells et al., 1987), and reflects alluviation on the plateau prior to regional incision of the gorge and the resulting drop of the water table.

Clay deposits exist locally, especially above Servilleta Basalt in the Los Cordovas fault zone, where they can be several meters thick. Some of these clays are lacustrine (Bauer and Kelson, 2004b) and likely formed in temporary lakes that formed behind lava dams. The lateral extents of the clays are generally unknown, although a distinctive light gray, clay layer is locally exposed in the walls of the Rio Grande gorge, just southwest of the study area, downstream from the confluence with the Rio Pueblo de Taos (unit Tlc in the cross sections). The clay is composed of very small (20 to 50 microns), well-sorted crystals of quartz and feldspar in a clay matrix that most likely formed in a lake that existed behind a basalt-dammed ancestral Rio Grande. The clay lies within

the clastic beds of the Lama formation, above the lowermost Servilleta Basalt, and is estimated to be 1 to 3 m thick. This clay layer has hydrologic significance. On the north slope of the gorge, between the Taos Junction bridge and Pilar, the clay is spatially related to a series of small springs and seeps that exist at elevations of approximately 6200 ft. The clay layer extends downstream, where it hosts a number of larger springs that emerge from the north gorge wall downstream from Pilar. The known, exposed lateral extent of the layer is a minimum of 17 km (11 mi) in the gorge. In addition, the clay likely extends up the Rio Pueblo de Taos, into the study area, where it is observed in several of the wells used in this study (TV-195, TV-196, TV-198).

Cuttings from deep exploration boreholes in the Taos area suggest the presence of the Tesuque Formation of the Santa Fe Group in the subsurface. From exposures near Pilar, and westward, and from along the upper Picuris piedmont, a general subsurface stratigraphy has been developed, although the sedimentary layers contain extensive vertical and horizontal compositional and textural variations due to the complex depositional environments found in the rift basin. The mappable members of the Tesuque Formation in the study area are the Chama-El Rito Member and Ojo Caliente Sandstone Member.

Along the western flank of the Picuris Mountains, the oldest Tesuque Formation unit is the Chama-El Rito Member, composed predominantly of volcanic-rich, non-fossiliferous sandstone and conglomerate, with minor mudrock interbeds. The Chama-El Rito Member represents braided stream deposits on a distal alluvial fan derived from a volcanic terrain to the northeast (Steinpress, 1980). Its thickness to the west of the study area was estimated to be 480 m (1,570 ft) (Steinpress, 1980).

The Chama-El Rito Member is conformably below, and interfingers with, the Ojo Caliente Sandstone Member of the Tesuque Formation west of the study area, along Rito Cieneguilla near Pilar (Leininger, 1982; Kelson et al., 1998). The Ojo Caliente is a buff to white, well-sorted eolian sandstone, consisting mostly of fine sand. Tabular crossbeds are common, with some sets over 4 m in height. Transport was from southwest to northeast (Steinpress, 1980). The Ojo Caliente is not exposed in the study area, but probably exists in the subsurface where it is likely thickly interbedded with the Chama-El Rito Member.

During the late Miocene, high-angle rift faulting produced deep, narrow, fault-bounded basins that filled with kilometers of clastic sediments and volcanic rocks. In the study area, the clastic sediments are named the Chamita Formation, and are principally composed of rounded to subrounded, pebble- to cobble-size clasts in a sand to silt matrix. The thickness of this basin fill is difficult to estimate at any given location. It is also difficult to distinguish in well logs from overlying Lama gravels and from underlying Chama-El Rito gravels. The Chamita Formation thickness was estimated to range from 100 to 230 m (330 to 750 ft) in the Pilar area (Steinpress, 1980).

### Picuris formation

The oldest known Cenozoic unit in the study area is the informal Picuris formation, a package of mostly volcaniclastic sedimentary rocks that represents pre-rift and early-rift sedimentation. Baltz (1978) stated that the early shallow rift basins of northern New Mexico were initially infilled by a combination of volcanic eruptions and volcaniclastic alluvial fans with sources in the San Juan volcanic field to the north. Rehder (1986) divided the Picuris formation into three members: a lower member, the Llano Quemado breccia member, and an upper member, on the basis of 11 scattered exposures north and east of the Picuris Mountains. Aby et al. (2004) utilized new geochronology, detailed regional mapping, and sedimentological analysis to refine the formation architecture, and their nomenclature is used in this report.

In the Picuris Mountains area, the Picuris formation consists principally of a variety of volcaniclastic sandstones and conglomerates, cobble/boulder conglomerates, colorful mudstones, siltstones, and sandstones, and a distinctive basal quartzite-boulder conglomerate. Based on geologic mapping along the northern Picuris Mountains piedmont, the transition from the upper Picuris formation to Tesuque Formation is probably gradational, although perhaps punctuated locally by unconformities.

In the Talpa area (Fig. 1), the Llano Quemado breccia is a monolithologic volcanic breccia of distinctive, extremely angular, poorly sorted, light-gray, recrystallized rhyolite clasts in a reddish matrix. Rhyolite clasts contain phenocrysts of biotite, sanidine, and quartz. A rhyolite clast yielded an $^{40}Ar/^{39}Ar$ eruptive age of 28.35 ±0.11 Ma (Aby et al., 2004).

### Older Tertiary volcanic rocks

Within the study area, one well (TV-100, RG-83352) penetrates a lava flow that is probably considerably older than the Servilleta Basalt. The drillers log lists “basalt” from 840 to 900 ft, and “fractured

basalt" from 900 to 920 ft. Given that geologic mapping shows the surface unit to be the Chama-El Rito Member of the Tesuque Formation (Miocene), the 80-ft-thick lava flow may be Oligocene in age. Such Oligocene lavas do exist at the surface north of the study area, where they are known as the Conejos Formation (ca. 30-29 Ma) and the Hinsdale Formation (ca. 26 Ma) (Thompson and Machette, 1989; Thompson et al., 1991). These lavas are related to the San Juan volcanic field, which predates the formation of the structural Rio Grande rift.

The Conejos Formation consists of andesite and dacite lava flows, flow breccias, lahar or mudflow breccias, and vent-facies pyroclastic rocks erupted or derived from local sources. The Hinsdale Formation consists of basaltic lava flows, associated breccia, and near-vent pyroclastic deposits (Thompson and Machette, 1989). Even though the Hinsdale Formation rocks are considerably older than the Pliocene rocks of the Taos Plateau volcanic field, the basalt-dominated Hinsdale can be quite similar in appearance to the younger Servilleta Basalt, and where the two formations are contiguous, they could be easily mistaken in borehole lithologic logs. The magnetic properties on this buried flow are different than the properties of the Servilleta lavas (Grauch et al., 2017).

### Paleozoic rocks

Most of the bedrock exposed in the Taos area east of the Rio Grande del Rancho consists of Paleozoic sedimentary strata of Mississippian and Pennsylvanian age. The Mississippian Tererro Formation of the Arroyo Peñasco Group contains mudstones, packstones, and crystalline limestone. The limestone contains calcitized evaporites and dolomites. All of the formation has undergone pervasive alteration. For detailed stratigraphic information on the Mississippian rocks of this region, see Armstrong and Mamet (1979, 1990).

In the Talpa area, the Tererro Formation is exposed near Ponce de Leon Springs (Plate 1), and presumably in the subsurface nearby, where it rests unconformably on the Proterozoic Miranda granite. Pennsylvanian strata exposed from the top of the Mississippian section on Cuchilla del Ojo near Ponce de Leon Springs eastward into the Sangre de Cristo Mountains are probably entirely Flechado Formation—a thick sequence of marine, deltaic, and continental sediments equivalent to part of the Madera Group to the south—although a series of large, north-striking faults have repeated and/or deleted parts of the section.

Although only a small portion of the study area contains Paleozoic rocks at the surface, it is likely that some of the area is underlain at depth by these rocks. Baltz and Myers (1999) proposed that the Pennsylvanian Taos trough actually continues northwestward near Taos, and that a thick section of Pennsylvanian rocks could underlie parts of the southern San Luis Basin. However, based on geologic mapping along the Picuris-Pecos fault system (Bauer et al., 2000), we believe that no significant thicknesses of Paleozoic strata exist west of the Miranda fault in the study area.

### Proterozoic rocks

The great variety of Paleoproterozoic and Mesoproterozoic rocks exposed in the Taos Range and Picuris Mountains exist in the subsurface of the San Luis Basin. In general, the Taos Range contains large areas of plutonic and gneissic complexes (including greenstones), whereas the northern Picuris Mountains are composed of metasedimentary rocks (quartzite, schist, phyllite) in fault contact with granite to the east. The eastern granite, known as the Miranda granite, is exposed in the ridges between Arroyo Miranda and Rio Grande del Rancho. For more information on the local Proterozoic rocks, see references cited in Montgomery (1953, 1963), Lipman and Reed (1989), Bauer (1988, 1993), and Bauer and Helper (1994).

## Faults of the Southern Taos Valley

Four major fault systems intersect in the study area:

1. Picuris-Pecos fault system;
2. Embudo fault zone;
3. Sangre de Cristo fault zone;
4. Los Cordovas fault zone.

### Picuris-Pecos fault system

Montgomery (1953) originally mapped the Picuris-Pecos fault in the Picuris Mountains. The fault has been traced for more than 60 km, from the northern Picuris Mountains, to near the village of Cañoncito, east of Santa Fe. The Picuris-Pecos fault system appears to have a long history of reactivation, probably from Proterozoic time to middle Tertiary time, although much of the net displacement appears to be Laramide-age dextral strike-slip movement (Bauer and Ralser, 1995).

In the study area, the Picuris-Pecos fault consists of five major, parallel north-striking fault zones (Fig. 3, Plate 1). From west to east, they are: Picuris-Pecos, La Serna, Miranda, McGaffey, and Rio Grande del Rancho faults. These faults are collectively referred to as the Picuris-Pecos fault system. Each fault zone consists of high-angle, anastomosing zones of distributed brittle shear in the Proterozoic and Paleozoic rocks. The major faults are located in valleys due to pervasive brittle deformational structures (fractures, fault gouge, fault breccia) that are relatively easily weathered and eroded. Following are short descriptions of each of the five fault zones. More detailed descriptions appear in Bauer et al. (1999) and Bauer and Kelson (2004b).

The Picuris-Pecos fault has experienced enough slip to juxtapose very different Proterozoic rock packages. West of the fault is the Hondo Group, a metasedimentary terrain of quartzite and schist. East of the fault is a distinctive medium-grained, orange-yellow granite (Miranda granite) that is similar in appearance to the granite exposed at Ponce de Leon Springs.

Approximately 1.3 km east of the Picuris-Pecos fault is the east-down La Serna fault, which has placed the Miranda granite on the west against the Picuris formation on the east (Bauer and Kelson, 2004b). The Picuris formation occupies a graben (Miranda graben) between La Serna fault and the west-down Miranda fault, located about 1.4 km to the east.

The main strand of the Miranda fault is inferred beneath Arroyo Miranda, based on water-well records and the juxtaposition of Picuris formation and Miranda granite. Good exposures in the Talpa/Llano Quemado area, where the Miranda fault zone cuts Picuris formation, display numerous north-striking, strike-slip faults with map separations measured on the order of meters to hundreds of meters. Notably, the <18 Ma upper Picuris formation is cut by high-angle faults with sub-horizontal slickenlines within the Miranda and La Serna fault zones, suggesting that Laramide-style, strike-slip faulting overlapped in time with development of the Rio Grande rift.

Approximately 1 km east of the Miranda fault is a set of west-down branching fault splays (the McGaffey fault) located on the bedrock ridge south of Talpa. The McGaffey fault offsets Proterozoic and Paleozoic rocks, but appears to have considerably less throw than adjacent fault zones. Strike-slip slickenlines are common on north-striking, high-angle minor fault planes. Notably, the high-discharge Ponce de Leon thermal springs are located at the intersection of the McGaffey, Miranda, and Embudo faults (Plate 1).

Approximately 1.5 km east of the McGaffey fault is the kilometer-wide, west-down Rio Grande del Rancho fault zone, a complex of branching faults along, and east of, the Rio Grande del Rancho valley. Most of the main strand of the fault zone is buried in the alluvial valley, but excellent exposures in the valley walls show extensive strike-slip breccia/fracture zones in Pennsylvanian strata.

### Embudo fault zone

The Embudo fault zone is a left-slip, north-down, oblique fault zone that forms the border between the west-tilted Española Basin and the east-tilted San Luis Basin of the Rio Grande rift (Fig. 2). The 64-km-long fault links the west-down southern Sangre de Cristo fault with the east-down Pajarito fault, and appears to be a high-angle fault with different senses of vertical separation along strike (Muehlberger, 1979; Leininger, 1982; Machette and Personius, 1984; Kelson et al., 1996, 1997, 2004a; Bauer and Kelson, 2004b).

The 36-km-long northern section, which includes the study area, was mapped in detail by Kelson et al. (1998), Bauer et al. (1997), and Bauer et al. (2000). Notably, the transition from the Embudo fault to the Sangre de Cristo fault is coincident with the Picuris-Pecos fault system. The northern Embudo fault is characterized by left-lateral slip (Muehlberger, 1979; Steinpress, 1980; Leininger, 1982; Kelson et al., 1997, 2004a). Along the northern margin of the Picuris Mountains, the mapped fault zone is over 2 km wide (Bauer et al., 1997), although aeromagnetic data demonstrate that buried, Embudo-style faults exist at least as far north as the Rio Pueblo de Taos (Fig. 5), thus increasing its width to as much as 9 km (5.6 mi) (Grauch et al., 2017). The northern Embudo fault shows evidence of displacement possibly as young as late Pleistocene or early Holocene. Muehlberger (1979) and Personius and Machette (1984) noted faulted Pleistocene alluvium in a road cut near the village of Pilar. Detailed mapping along the fault showed additional evidence of late Pleistocene displacement, and identified two localities where young, possibly early Holocene alluvial fans may be faulted.

In Proterozoic bedrock units, the major strands of the Embudo fault are well-developed, high-angle, brittle deformation zones. Some are many tens of meters wide, typically consisting of central zones of intense strain (breccia, fault gouge, closely spaced fractures) flanked by wide zones of fractured rock.

Fractures typically are open, with only minor carbonate cementation. Commonly, the massive sandstone and conglomerate beds contain thoroughgoing fractures, whereas the interlayered, more ductile, shales are unfractured. Tracing the fault zone eastward into the Cañon section of the Sangre de Cristo fault, slickenlines plunge steeper and steeper until they are down dip on the west-dipping Sangre de Cristo fault.

Where the fault is exposed in Tertiary rocks, the bedrock has been reduced to a clay-rich fault gouge that contains a strong tectonic foliation that indicates the sense of shearing. Moving away from the fault plane, the gouge zones grade into altered and fractured bedrock, and then into relatively unstrained country rock. Where the faults cut Quaternary deposits, the alluvium is laced with thin, anastomosing, calcite-filled fracture veins. Alteration zones are common, and gravel clasts are rotated into the foliation plane. However, the overall degree of deformation is considerably less in the Quaternary deposits than in older units.

### Sangre de Cristo fault zone

The Sangre de Cristo fault zone is a west-dipping normal fault zone that forms the border between the Sangre de Cristo Mountains on the east and the San Luis Basin on the west. The southern Sangre de Cristo fault within Colorado and New Mexico is divided into five primary sections (Menges, 1988; Machette et al., 1998). From north to south, these are the San Pedro Mesa, Urraca, Questa, Hondo, and Cañon sections (Machette et al., 1998). The southernmost Cañon section strikes about N20°E, and extends south from the Rio Pueblo de Taos to the Rio Grande del Rancho, where it becomes the Embudo fault. Together, the Hondo and Cañon sections of the southern Sangre de Cristo fault border a 30-km-long, 10-km-wide, crescent-shaped re-entrant in the Sangre de Cristo range block, informally referred to as the Taos embayment (Fig. 2).

The southernmost Sangre de Cristo fault shows prominent geomorphic evidence of late Quaternary surface rupture, including scarps across alluvial fans of various ages, air-photo lineaments, springs, and alignments of vegetation. Machette and Personius (1984) and Personius and Machette (1984) profiled several scarps along the Cañon section, and suggested a Holocene age for the most-recent movement. Kelson (1986) mapped late Quaternary deposits and some fault strands along this section, and showed faulted late Pleistocene alluvial-fan deposits. Menges (1990) conducted detailed morphometric analyses of the range front and fault scarps, and suggested the possibility of early Holocene to latest Pleistocene movement along the Cañon section. Recent geologic mapping (Bauer et al., 2000, Bauer and Kelson, 2001) and fault trenching (Kelson et al., 2004b) supported these previous age estimates.

Geologic mapping has shown that the southernmost Sangre de Cristo fault zone is a complex system of branching faults that is at least 2 km wide (Bauer and Kelson, 2001). With the exception of the Rio Fernando de Taos area, fault scarps in Quaternary deposits are mostly confined to the mountain front where Quaternary deposits are in fault contact with Pennsylvanian rocks. Individual fault planes typically dip steeply west to northwest, with slickenlines plunging moderately to steeply westward.

The transition from strike-slip to dip-slip is gradational, with a prevalence of oblique-slip (plus some strike-slip) faults in the bedrock just southeast of Talpa. In Pennsylvanian rocks near the Rio Grande del Rancho, faults dip between 60 and 80° northwest with moderately west-plunging slickenlines. North of the Rio Fernando, faults dip between 70 and 89° westward with generally down-dip slickenlines.

### Los Cordovas fault zone

Previous workers described a 5- to 8-km-wide zone of north-striking faults in the Taos Plateau (Lambert, 1966; Machette and Personius,1984). The Los Cordovas fault zone consists of perhaps 10 or more individual fault strands that generally are about 10 km long and have fairly regular spacings of 1-1.5 km. The western margin of the fault zone is roughly coincident with the Rio Grande gorge. Where separation is greatest, these west-down faults juxtapose piedmont-slope alluvium against older Servilleta Basalt.

Machette and Personius (1984) reported that the fault offset is greater than the 15- to 30-m-high erosional scarps that now define the surface expression, and that faulting may be as old as early Pleistocene, but could be as young as middle(?) Pleistocene. Profiles of stream terraces along the Rio Pueblo de Taos suggest that the faults displace the early(?) to middle Pleistocene piedmont surface, but not a middle Pleistocene terrace (Kelson, 1986; Machette et al., 1998). Geologic mapping suggests that these faults may extend southward from the Rio Pueblo de Taos, and may deform high alluvial-fan deposits on the Picuris piedmont (Bauer and Kelson, 2004b). In addition, the high-resolution aeromagnetic map of the study area may show some evidence for buried

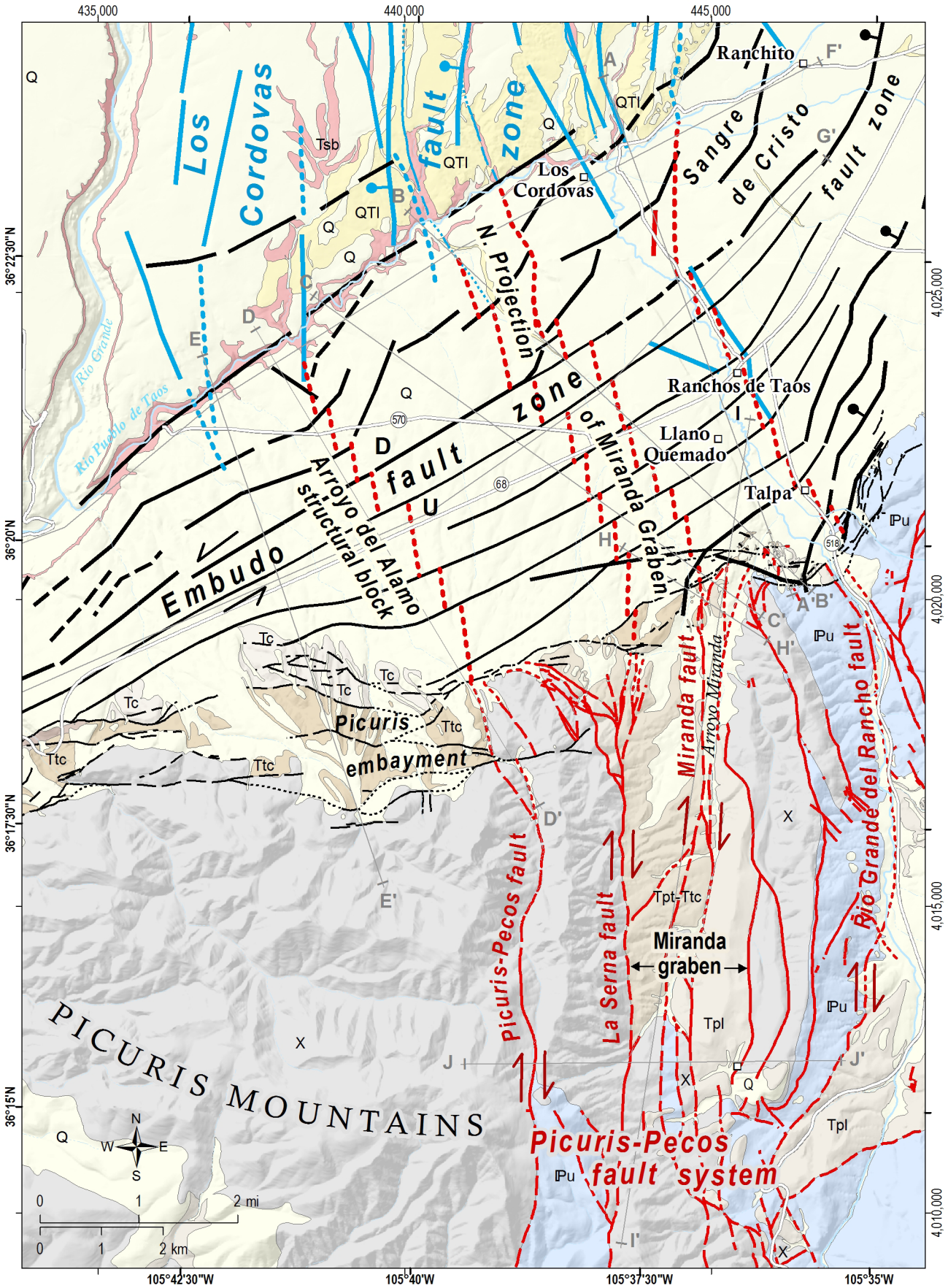


**Figure 5.** Structural model of the regional fault systems in the southern Taos Valley. Picuris-Pecos fault system shown in red. Embudo and Sangre de Cristo fault zones shown in black. Los Cordovas fault zone shown in blue. Each fault system is coded according to whether the fault segments are mapped, deduced by geophysical methods, or inferred from the geologic model. See Appendix 1 for geologic unit descriptions.

## Geologic units

| | |
|---|---|
| Q | *Quaternary deposits* |
| QTl | *Lama formation* |
| Tsb | *Servilleta Basalt* |
| Tc | *Chamita Formation* |
| Tto | *Ojo Caliente Sandstone mbr.* |
| Ttc | *Chama - El Rito Mbr.* |
| Tpt-Ttc | *Picuris formation - Chama-El Rito Mbr.* |
| Tpl | *Picuris formation, lower mbr.* |
| PPu | *Paleozoic rocks* |
| X | *Proterozoic rocks* |

## Explanation of faults

**Embudo fault system** - Mostly east-to-northeast striking, north-down, left-oblique, high-angle, normal faults in units of all ages. Represents an antithetic transfer zone between the San Luis and Española rift basins. Transitions to west-down normal faults of the Sangre de Cristo fault system in the eastern study area.

Mapped. Dashed where approximately located; dotted where concealed.

Inferred from gravity model. All locations are approximate.

Inferred from high-resolution aeromagnetic data. Dashed where lower certainty.

**Los Cordovas fault zone** - Mostly northerly striking, west-down normal faults in rift-related units. At depth, these faults may merge with Laramide faults of the Picuris-Pecos fault system.

Mapped. Dashed where approximately located; dotted where concealed.

Inferred from high-resolution aeromagnetic data. Dashed where lower certainty.

**Picuris-Pecos fault system** - Mostly northerly striking, dextral, strike-slip faults in Proterozoic and Paleozoic rocks. Principally related to the Laramide orogeny, but likely deformed some of the older pre-rift (Oligocene) rocks of the Picuris formation.

Mapped. Dashed where approximately located; dotted where concealed.

Inferred from conceptual geologic model of Bauer and Kelson (2004).

Inferred from high-resolution aeromagnetic data.

U D Fault showing local offset, U = upthrown block, D = downthrown block

Fault, ball and bar on downthrown block

Fault, arrows show relative motion

structural links between the Picuris-Pecos fault system and Los Cordovas faults.

An excellent exposure of the eastern fault strand was found just north of the Rio Pueblo in an arroyo that cuts across the fault scarp. In the exposure, Servilleta Basalt and overlying Quaternary fan deposits are faulted on a plane that dips 45° west with down-dip slickenlines and rotated cobbles. Overlying Holocene colluvial gravels are not faulted. A distinctive red to yellow faulted clay horizon rests on the basalt. Laboratory analysis has shown that the clay probably represents a lake deposit that was derived from altered volcanic rocks (G. Austin, written communication, 2001).

### Taos graben

The Taos graben, first recognized by Cordell (1978) from gravity data, is a major structural feature in the southeastern San Luis Basin. The latest geophysical model (Grauch et al., 2017) substantially refines the shape of the Taos graben, depicting a deep, slightly asymmetrical "Taos subbasin" just north of our study area. At the latitude of Taos, the Taos subbasin is a crescent-shaped feature that contains approximately 1800 m (5900 ft) of basin fill in its deepest region just north of our study area (Grauch et al., 2017). The deep subbasin extends southwestward under the Rio Pueblo de Taos, nearly to the Rio Grande confluence. Grauch et al. (2017) concluded that the Taos subbasin represents the cumulative fault activity on the Embudo fault zone and Sangre de Cristo fault system since rift inception at about 25 Ma.

In 1996, the "Town Yard" exploration well was reported to have encountered Pennsylvanian limestone, shale, and sandstone from a depth of 720 ft to the bottom of the hole at 1020 ft (Drakos et al., 2004a). If correct, this would have pinned the eastern structural edge of the Taos graben between that well and the 2100-ft-deep BOR-3 well, which was drilled about 1 km to the west. This would have required a structural bench with relief of more than 1400 ft between the two wells. However, recent geophysical analyses (Grauch et al., 2017) and petrographic analysis of well cuttings (D. Koning, written commun., 2013) concluded that the Town Yard well did not drill into Paleozoic bedrock, but instead penetrated conglomeratic basin-fill rocks, and therefore the eastern edge of the deep, inner graben lies farther to the east.

The Taos graben was mostly formed by the time the oldest Servilleta Basalt erupted, approximately 5 Ma. On the Taos Plateau, the Rio Grande

was superposed on the plateau after eruption of the youngest Servilleta Basalt (circa 2.8 Ma), and began to rapidly entrench upon integration of the river system at approximately 0.5 Ma (Wells et al., 1987). Some of the high-angle faults on the plateau appear to have caused thickening and thinning of volcanic flows across the faults. North of the map area, an example of basalt thinning is exposed at the Dunn Bridge fault, where the thickness of the sedimentary interval between the middle and upper basalts varies 17 m (56 ft) across the fault.

### Miranda graben

The Miranda graben is formed between two sections of the Picuris-Pecos fault system, the west-down Miranda fault to the east and the east-down La Serna fault to the west. In the study area, the graben is approximately 1.6 km (1.0 mi) wide and is filled with sedimentary rocks of the Picuris formation that are in fault contact with Proterozoic granites to the east and west (Fig. 3). In the Ponce de Leon neighborhood, water wells indicate that 300 to 400 ft of lower Picuris formation overlies Proterozoic granite and quartzite. At its northernmost exposure near Ponce de Leon, the graben is transected by numerous strands of the Embudo fault zone. Although the graben certainly exists buried beneath rift-fill sediments to the north of Ponce de Leon, it will be highly segmented and offset by the north-down, left-slip movement along Embudo fault strands. Ponce de Leon Springs is located at the east edge of the Miranda graben, where several strands of the Miranda and Embudo faults intersect.

### Picuris embayment

In the central study area, just west of the Picuris-Pecos fault, the contact between the basin-fill units and the Proterozoic rocks along the north flank of the Picuris Mountains delineate an indentation, named the "Picuris embayment" (Fig. 5, Plate 1). The embayment is about 3 km across (east-west) and 1 km deep (north-south), and is filled with rocks of the Chama-El Rito Member, which either onlap the basement rocks, or are faulted against them, or both. Several mappable splays of the Embudo fault zone cross the area, and the strata of the Chama-El Rito are tilted at least up to 45o, indicating that the basin-fill rocks have been strongly affected by the faults. A combination of movement along the Picuris-Pecos fault (and perhaps other unidentified north-striking faults along the western edge of the embayment) and younger movement along the Embudo fault strands was likely responsible for the development of the embayment.

The only water well (TV-100) identified in the embayment was drilled through basin-fill sediments until encountering "quartz" (interpreted as at, or just above, Proterozoic bedrock) at 920 ft depth. As interpreted in cross sections D-D' and E-E' (Plate 2), the Picuris embayment is a zone in which the older basin-fill units (Tp and Ttc) are inset into the flank of the Picuris Mountains on a shallow basement bench.

The Picuris-Pecos fault continues northward under the Picuris piedmont, and likely links up with a major, buried strand of the Los Cordovas fault zone near the Rio Pueblo de Taos (Fig. 5). Because the Picuris-Pecos fault is older than the Embudo fault zone, our fault model also shows multiple zones of segmentation of the buried Picuris-Pecos fault as it crosses each strand of the Embudo fault zone. The section of the Picuris-Pecos fault that is buried under the Picuris piedmont has caused major offset of the Proterozoic rocks, but only moderate offset of the basin-fill rocks as it merges upward with the buried Los Cordovas fault (Plate 2).

The area of the Picuris piedmont that is bordered by the Picuris embayment to the south, the Picuris-Pecos/Los Cordovas fault trace to the east, and the Rio Pueblo de Taos to the north, is referred to as the "Arroyo del Alamo structural block" (Fig. 5). This fault-bounded block displays some unique hydrogeologic conditions that are thought to be the result of the characteristics of the faulted basin-fill deposits (Johnson et al., 2016).

The projection of the Picuris-Pecos/Los Cordovas fault to the Rio Pueblo de Taos also corresponds with a major river knickpoint. Above the fault intersection, the river gradient is low (36 ft/mi) and the channel is broad. Below the fault intersection, the gradient is high (151 ft/mi), and the river has carved a steep canyon through the basalts to its confluence with the Rio Grande. Our preferred working hypothesis is that the buried fault is a steeply dipping normal fault, and the footwall block of upper Servilleta Basalt has created the river knickpoint.

## Conceptual Structural Model

Figure 5 is a simplified geologic map that illustrates our conceptual model for the major fault zones in the study area. For each of the fault zones (Picuris-Pecos in red; Embudo and Sangre de Cristo in black; Los Cordovas in blue), we show their mapped faults,

aeromagnetic faults, and inferred faults. The Picuris-Pecos faults are oldest, and are visualized in the rift basin as being offset in a north-down/left-slip sense by the younger Embudo fault strands. The Picuris-Pecos faults are restricted to the bedrock (Proterozoic, Paleozoic, and the older Picuris formation). The intersection of these two fault systems therefore divides these older units into complex, fault-bounded polygons. The Embudo fault zone also interacts with the young Los Cordovas faults in some complex manner, especially in areas where the zone fault systems overlap in time. However, these two fault systems will have predominantly divided the basin-fill units (younger Picuris formation and Santa Fe Group) into complex, fault-bounded polygons. The net result of this complex structural model is a highly heterogeneous stratigraphy that has profound effects on the groundwater systems in the study area (Johnson et al., 2016).

### Geometry of buried faults

Because the Picuris-Pecos faults are cut by the Embudo fault, they predate the Embudo system and, importantly, most likely exist in the subsurface north of the active Embudo fault. Because the older members of the Picuris formation are restricted to the structurally low areas within the fault system, Bauer and Kelson (2004b) suggested that the Picuris-Pecos fault zone defined the Eocene(?) to early Miocene grabens, which served as loci for deposition of volcaniclastic sediments of the Picuris formation that were shed southward from the San Juan volcanic highlands. At least part of the Miranda graben has remained low during the last 25 Ma, thus preserving rocks of the Picuris formation. Therefore, the grabens are generally older than the Embudo fault system, and the graben-bounding faults most likely extend northward into the basin. If so, the Picuris formation rocks exist on the northern side of the Embudo fault, beneath Santa Fe Group sediments in the study area.

In an evaluation of the major fault systems of the study area, Bauer and Kelson (2004b, p. 144) stated: "*In summary, the three major fault systems in the Taos area are more geometrically complex than described in previous literature. The Picuris-Pecos fault is actually only the western strand of an 8-km-wide brittle deformational zone herein named the Picuris-Pecos fault system. The fault system is a repeatedly reactivated crustal flaw that was a locus for south-transported Laramide volcaniclastic sediments from about 35 Ma (Picuris formation) to 18 Ma (Tesuque Formation), and possibly later. The faults most likely exist in the basement of the basin west of Taos. The Pleistocene Los Cordovas faults may be westward transported, growth-fault remnants of the Picuris-Pecos fault system. The Picuris-Pecos faults may also define the structural boundaries of the Taos graben. The Picuris-Pecos fault system is truncated by the Embudo transfer fault, which merges into the Sangre de Cristo fault. During early extension, prior to development of the Embudo fault, the Picuris-Pecos fault system, and its now-buried northward extension, may have represented the eastern rift margin along with the Questa section of the Sangre de Cristo fault and the Town Yard fault. At some later time (mid- Miocene?), as the Embudo transfer fault developed, the Sangre de Cristo fault jumped eastward to the Cañon and Hondo sections, forming the Taos embayment …*"

These fault relationships are illustrated in the geologic cross sections (Plate 2) and the geologic fault model map (Fig. 5). In the cross sections, the principal elements of the Picuris-Pecos fault system only cut rocks as young as the Picuris formation, and then shallow into the younger, rift-related Los Cordovas normal faults. The Embudo fault system cuts both the older rocks affected by the Picuris-Pecos faulting, and the young basin fill, and the faults are consistently north-down, left-oblique into the basin.

### 3D patterns of basin-fill units

Although much of the Picuris piedmont is covered by thin alluvial deposits, the underlying Tertiary sedimentary units are well enough exposed to display some general patterns that are the result of the interaction of movement along the Embudo faulting and the primary depositional settings of some of the units. In general, the oldest sedimentary units (Picuris formation, Chama-El Rito Member) crop out along the mountain front, whereas the younger units (Ojo Caliente Sandstone Member, Chamita Formation, Lama formation) exist only to the north along the middle to lower parts of the piedmont slope (Plate 1).

Picuris formation rocks were deposited on pre-rift bedrock (Paleozoic and Proterozoic rocks). Due to displacements along the Embudo fault zone, the Picuris formation is now preserved around much of the flank of the Picuris Mountains. In the study area, the Picuris formation is exposed at the surface east of the Picuris-Pecos fault, but not exposed at the surface west of the Picuris-Pecos fault. However, borehole data do indicate that Picuris formation rocks exist in the subsurface west of the fault. Presumably, the Picuris formation also extends northward into the rift

basin, where it is consecutively dropped down along a series of large-displacement, north-down Embudo faults (Fig. 5; Plate 2).

The Chama-El Rito Member (Ttc) occurs along much the upper Picuris piedmont (Plate 1). Locally, where it has been eroded from the uplifted Picuris Mountains, it may exist as only a thin layer atop the Picuris formation. Aby et al. (2004) concluded that the uppermost Picuris formation grades into the overlying Chama-El Rito Member of the Tesuque Formation, and therefore the exact location of the contact is indistinct. Presumably, the Chama-El Rito Member also extends northward into the rift basin, where it is consecutively dropped down along the series of large-displacement, north-down Embudo faults.

In the study area, the Ojo Caliente Sandstone Member (Tto) is only exposed in the westernmost exposure of the Embudo fault zone, along NM-68 (Plate 1). However, based on borehole analysis, Glorieta Geoscience, Inc. (2007) concluded that it underlies a significant part of the southern rift basin. In our subsurface model, we show the unit thinning to the south and east as the migrating sand dunes would have begun to encounter the active Embudo and Sangre de Cristo fault scarps. Thus, within the study area, the Ojo Caliente is missing or very thin under the southern and eastern parts of the Picuris piedmont. Additionally, because it is also down dropped northward into the rift basin along medium-displacement faults, significant thicknesses of shallow Ojo Caliente are limited to the central zone of the Picuris piedmont.

Based on borehole analysis in the study area, Glorieta Geoscience, Inc. (2007) defined a stratigraphic unit that is transitional between the eolian sandstone of the Ojo Caliente Sandstone Member and the conglomeratic sandstones of the Chamita Formation. We have retained that unit as "Tto & Tc" on the cross sections (Plate 2). Its distribution in the study area is similar to that of the Ojo Caliente.

The Chamita Formation (Tc) is not exposed in the study area, although excellent exposures exist on the south side of Pilar Mesa, just west of the study area. The Chamita was locally derived from the Picuris and Sangre de Cristo Mountains, and exists in the shallow subsurface throughout the study area, except where it has been eroded from the upper Picuris piedmont. Although the Chamita is dropped down into the rift basin by Embudo faults, the fault offsets are typically less than 200 feet, and so Chamita deposits likely underlie much of the study area at shallow levels.

The Lama formation was derived mainly from the Sangre de Cristo Mountains to the east, and it now exists at or near the surface over much of the northeastern part of the study area. In the stratigraphic model shown in Plate 2, approximately halfway up the Picuris piedmont, the Lama formation merges into equivalent uppermost Chamita Formation alluvial fans that prograded northward from the Picuris Mountains. The location of the contact between the Lama and Chamita is approximate, and certainly represents an interfingering of the two deposits over considerable distances and in complex ways.

**Southern extent of basalt**

Aeromagnetic and borehole analysis make it possible to accurately define the extent of Servilleta Basalt in the subsurface of the study area. The surface projection of this zone is shown on the geologic map as a red line labeled "southern extent of basalt" (Plate 1). In the geologic cross sections (Plate 2), the basalt flows terminate southward on a major, buried splay of the Embudo fault. The coincidence of the fault and the lava flow terminations can be placed with high confidence due to the interpretations of the high-resolution aeromagnetic data (Grauch et al., 2015, 2017). In general, the number of basalt-flow packages, and their thicknesses, decrease southward as they approach the buried fault splay. Embudo fault scarps may have created topographic barriers to the prograding lava flows during Pliocene time, and the lava flows may have later been offset by fault scarps, and then eroded from the footwalls.

In the Los Cordovas area, near the confluence of the Rio Pueblo de Taos and Rio Grande del Rancho, there exists a ~1-km-wide domain where the basalt flows show a wide range of abrupt thickness changes, including areas where the Servilleta Basalt ranges from zero to several hundred feet thick over short distances. The controls on basalt thicknesses in this area are unknown, but probably involve some combination of fault scarp dams, other paleotopography, and later erosion of basalts.

## Summary of the Geologic System

1. The study area is located in the southeast corner of the San Luis Basin of the Rio Grande rift, and includes stratigraphic and structural elements of the rift, the Taos Plateau volcanic field, and the southern Rocky Mountains.

These elements combine to create an extremely complex geologic setting with a diversity of rock types and ages that is overprinted by a long history of tectonism, volcanism, sedimentation, and erosion.

2. The study area contains rocks and deposits that range in age from Paleoproterozoic (1.7 billion years old) to Holocene. Proterozoic crystalline rocks and Paleozoic sedimentary rocks are exposed in the Picuris and Sangre de Cristo Mountains, and presumably also exist buried within the rift basin. The oldest Tertiary sedimentary rocks (Picuris formation) represent pre-rift to early-rift deposition, and are found in Laramide grabens (Miranda and Rio Grande del Rancho grabens) and buried in the rift basin. The youngest Tertiary sedimentary rocks (Santa Fe Group) are found only in the rift basin, where they were deposited in a complex three-dimensional package that ranges up to at about 1800 m (5900 ft) thick. The only volcanic rocks exposed in the area are packages of thin, basaltic, Pliocene lava flows (Servilleta Basalt) that flowed into the study area from the northwest. The youngest units in the study area are thin, unconsolidated, alluvial and colluvial sheets of surficial deposits that cover much of the rift basin.
3. Clay deposits appear to be common in the basin-fill sediments. Analyses of several clays suggest that they are laterally extensive and may have formed in temporary shallow lakes that formed behind lava dams. A 2-m-thick clay in the western study area is clearly related to a number of perched seeps and springs that exist on the canyon walls of the Rio Grande gorge.
4. Four major zones of faults intersect in the southern Taos Valley. The oldest, the Picuris-Pecos fault system, consists of multiple, north-striking, high-angle, dextral strike-slip faults that offset rocks as young as the Picuris formation in the eastern Picuris Mountains. The Sangre de Cristo and Embudo fault zones flank the edge of the Rio Grande rift, and have dropped down rocks of all ages into the rift basin. Both of these rift-flanking fault zones are considerably wider than their mapped exposures; at least several kilometers wide beneath the piedmont slopes that surround the basin. The Los Cordovas fault zone consists of several small-displacement, west-down, normal faults in the northern study area. All of these fault systems consist of geometrically complex fault planes that branch, merge, curve, and terminate in three dimensions. Out of necessity, our geologic cross sections are intentionally simplified in order to be able to show the general geometries and kinematics of the major faults.
5. The Miranda graben of the Picuris-Pecos fault system is formed between the west-down Miranda fault and the east-down La Serna fault. In the study area, it is filled with sedimentary strata of the Picuris formation that overlie crystalline basement rocks. The graben is truncated by the Embudo fault system, but certainly exists in the subsurface of the rift basin where it presumably is progressively offset by each of the north-down, left-oblique Embudo fault strands.
6. The hot spring system, Ponce de Leon Springs, is located at the intersection of several fault splays along the eastern edge of the Miranda graben. Other thermal springs in the region (Manby Hot Springs, Black Rock, unnamed spring near Taos Junction bridge) are also located on faults.
7. The four fault zones in the study area overlap in various ways in time and space. Our geologic model states that the Picuris-Pecos fault system exists in the basement rocks (Picuris formation and older units) of the rift, where it is progressively down dropped and offset to the west by each Embudo fault strand between the Picuris Mountains and the Rio Pueblo de Taos. In this model, the Miranda graben exists in the subsurface as a series of offset basement blocks between the Ponce de Leon neighborhood and the Town of Taos well field. In the study area, the Embudo faults are pervasive structures between the Picuris Mountains and the Rio Pueblo de Taos, affecting all geologic units that are older than the Quaternary surficial deposits. The Los Cordovas faults are thought to represent the late Tertiary to Quaternary reactivation of the old and deeply buried Picuris-Pecos faults. If so, then the Los Cordovas may extend southward under the Picuris piedmont, where they exist as growth faults as they merge downward into the reactivated(?) Picuris-Pecos faults. If the Los Cordovas and Picuris-Pecos faults are interconnected in this way, they would be likely to facilitate upward flow of deep fluids into shallow aquifer zones, such as at Ponce de Leon Springs.
8. Exposures of Picuris-Pecos and Embudo faults in some bedrock units (Proterozoic rocks, Paleozoic sandstones and carbonates) show severe fracturing and brecciation of the rocks,

producing high-permeability zones in the rocks. In contrast, rare exposures of faults in the basin-fill units (Santa Fe Group, other than Ojo Caliente Sandstone Member) show clay-filled damage zones that would likely decrease lateral permeabilities across high-angle faults, and create water-bearing domains and compartments in the basin-fill aquifers.

9. The exceptionally high density of cross-cutting faults in the study area has severely disrupted the stratigraphy of the Picuris formation and the Santa Fe Group. The Picuris formation exists at the surface in the Miranda and Rio Grande del Rancho grabens, and locally along the top of the Picuris piedmont. In the subsurface, the Picuris formation deepens rapidly from the mountain front into the rift basin. In a similar manner, the Tesuque and Chamita Formations are shallowly exposed close to the mountain front, but are down dropped into the basin along the Embudo faults. The Ojo Caliente Sandstone Member of the Tesuque Formation appears to be thickest in the northwestern part of the study area, and thins toward the south and the east. In the study area, the Lama formation thins westward and southward. The Servilleta Basalt is generally thickest to the north and northwest, thins under the Picuris piedmont, and terminates along an extraordinarily linear, buried strand of the Embudo fault zone, suggesting that these lava flows were temporally related to Embudo fault activity.
10. Our geologic model shows a thick section of Paleozoic rocks to the east, with a general thinning trend westward until the section is truncated by the Miranda fault. In our model, no appreciable thickness of Paleozoic strata exists in the rift basin west of the projection of the Miranda fault northward to the Rio Pueblo de Taos.
11. The Picuris embayment is an indentation along the Picuris Mountains range front in the central part of the study area, just west of the Picuris-Pecos fault and Arroyo del Alamo. The embayment is filled with Tesuque Formation rocks that overlie basement units. The area between the Picuris embayment to the south, the projection of the Picuris-Pecos fault to the east, and the Rio Pueblo de Taos to the north is called the Arroyo del Alamo structural block. The northeast corner of this structural block corresponds with a strand of the Los Cordovas fault zone, and an abrupt gradient change on the Rio Pueblo de Taos. The gradient change is interpreted as a river knickpoint that was created by the offset of the uppermost Servilleta Basalt layer by a west-down Los Cordovas fault.

# ACKNOWLEDGMENTS

Project funding came from the New Mexico Bureau of Geology and Mineral Resources, U.S. Geological Survey (USGS), Taos County, and the Healy Foundation. Paul Drakos, Jim Riesterer, and Megan Hodgins (Glorieta Geoscience, Inc.) were exceptionally helpful by providing information on the wells and subsurface geology of the area. Peter Vigil, Dr. Tony Benson, and Ron Gervason (Taos Soil & Water Conservation District) and Kylian Robinson (UNM Taos) provided locations of some water wells in the study area. Dr. Ren Thompson (USGS, Denver) shared his expertise on the geology of the Taos Plateau volcanic field. Maryanne Wasiolek (Hydroscience Associates, Inc.) provided information on the exploratory water wells in Miranda Canyon. Michael Darr kindly shared his knowledge of the subsurface hydrogeologic conditions of the Llano Quemado area. We thank Adam Read (NMBGMR) and Christine Chan (USGS) for their insightful and valuable technical reviews. Any use of trade, firm, or product names is for descriptive purposes only and does not imply endorsement by the U.S. Government.

# REFERENCES


Aby, S.B., Bauer, P.W., and Kelson, K.I., 2004, The Picuris formation: A late Eocene to Miocene sedimentary sequence in northern New Mexico, in Brister, B.S., Bauer, P.W., Read, A.S., and Lueth, V.W., eds., Geology of the Taos Region: New Mexico Geological Society, 55th Annual Field Conference Guidebook, p. 335-350.

Aby, S.B., Hallet, B., and Bauer, P.W., 2007, Geologic map of the Tres Ritos quadrangle, Taos County, New Mexico: New Mexico Bureau of Geology and Mineral Resources Open-File Geologic Map 145, scale 1:24,000.

Appelt, R.M., 1998, 40Ar/39Ar geochronology and volcanic evolution of the Taos Plateau volcanic field, northern New Mexico and southern Colorado [M.S. thesis]: Socorro, New Mexico Tech, 58 p.

Armstrong, A.K., and Mamet, B.L., 1979, The Mississippian system of north-central New Mexico, in Ingersoll, R.V., Woodward, L.A., James, H.L., eds., Santa Fe Country: New Mexico Geological Society, 30th Annual Field Conference Guidebook, p. 201–207.

Armstrong, A.K., and Mamet, B.L., 1990, Stratigraphy, facies, and paleotectonics of the Mississippian system, Sangre de Cristo Mountains, New Mexico and Colorado and adjacent areas, in Bauer, P.W., Lucas, S.G., Mawer, C.K., and McIntosh, W.C., eds., Tectonic Development of the Southern Sangre de Cristo Mountains, New Mexico: New Mexico Geological Society, 41st Annual Field Conference Guidebook, p. 241–249.

Baltz, E.H., 1978, Resume of Rio Grande depression in north-central New Mexico, in Hawley, J.W., ed., Guidebook to Rio Grande rift in New Mexico and Colorado: New Mexico Bureau of Mines and Mineral Resources Circular 163, p. 210-228.

Baltz, E.H., and Myers, D.A., 1999, Stratigraphic framework of upper Paleozoic rocks, southeastern Sangre de Cristo Mountains, New Mexico, with a section on speculations and implications for regional interpretation of Ancestral Rocky Mountains paleotectonics: New Mexico Bureau of Geology and Mineral Resources Memoir 48, 272 p.

Bankey, V., Grauch, V.J.S., and Fugro Airborne Surveys Corp., 2004, Digital aeromagnetic data and derivative products from a helicopter survey over the Town of Taos and surrounding areas, Taos County, New Mexico: U.S. Geological Survey Open-file Report 2004-1229A, CD-ROM. http://pubs.usgs.gov/of/2004/1229/A/

Bankey, V., Grauch, V.J.S., Webbers, A., and PRJ, Inc., 2005, Digital data and derivative products from a high-resolution aeromagnetic survey of the central San Luis Basin, covering parts of Alamosa, Conejos, Costilla, and Rio Grande Counties, Colorado, and Taos County, New Mexico: U.S. Geological Survey Open-file Report 2005-1200, available at http://pubs.usgs.gov/of/2005/1200/.

Bankey, V., Grauch, V.J.S., Drenth, B.J., and Geophex, Inc., 2006, Digital data from the Santa Fe East and Questa-San Luis helicopter magnetic surveys in Santa Fe and Taos Counties, NM, and Costilla County, Colorado: U.S. Geological Survey Open-File Report 2006–1170, 4 p. with maps; online only at http://pubs.usgs.gov/of/2006/1170/.

Bankey, V., Grauch, V.J.S., Drenth, B.J., and EDCON-PRJ Inc., 2007, Digital data from the Taos West aeromagnetic survey in Taos County, New Mexico: U.S. Geological Survey Open-File Report 2007-1248, http://pubs.usgs.gov/of/2007/1248/

Bauer, P.W., 1988, Precambrian geology of the Picuris Range, north-central New Mexico, [Ph.D. thesis]: New Mexico Bureau of Geology and Mineral Resources Open-File Report OF-325, 260 p.

Bauer, P.W., 1993, Proterozoic tectonic evolution of the Picuris Mountains, northern New Mexico: Journal of Geology, v. 101, p. 483-500.

Bauer, P.W., and Helper, M., 1994, Geology of the Trampas 7.5-minute quadrangle, Taos County, New Mexico: New Mexico Bureau of Mines and Mineral Resources Geologic Map GM-71, scale 1:24,000.

Bauer, P.W., and Kelson, K.I., 2001, Geologic map of the Taos 7.5-minute quadrangle, Taos County, New Mexico: New Mexico Bureau of Geology and Mineral Resources Open-File Geologic Map 43, scale 1:24,000.

Bauer, P.W., and Kelson, K.I., 2004a, Rift extension and fault slip rates in the southern San Luis Basin, New Mexico, in Brister, B.S., Bauer, P.W., Read, A.S., and Lueth, V.W., eds., Geology of the Taos Region: New Mexico Geological Society, 55th Annual Field Conference Guidebook, p. 172-180.

Bauer, P.W., and Kelson, K.I., 2004b, Cenozoic structural development of the Taos area, New Mexico, in Brister, B.S., Bauer, P.W., Read, A.S., and Lueth, V.W., eds., Geology of the Taos Region: New Mexico Geological Society, 55th Annual Field Conference Guidebook, p. 129-146.

Bauer, P.W., Kelson, K.I., and Aby, S.B., 1997, Geology of the Taos SW 7.5-minute quadrangle, Taos County, New Mexico: New Mexico Bureau of Geology and Mineral Resources Open-File Geologic Map 12, scale 1:24,000.

Bauer, P.W., and Ralser, S., 1995, The Picuris-Pecos fault–repeatedly reactivated, from Proterozoic(?) to Neogene, in Bauer, P.W., Kues, B.S., Dunbar, N.W., Karlstrom, K.E., Harrison, B., eds., Geology of the Santa Fe Region: New Mexico Geological Society, 46th Annual Field Conference Guidebook, p. 111-115.

Bauer, P.W., Johnson, P.S., and Kelson, K.I., 1999, Geology and hydrogeology of the southern Taos Valley, Taos County, New Mexico: Technical report for the New Mexico Office of the State Engineer: New Mexico Bureau of Geology and Mineral Resources Open-File Report 501, 80 p., with 4 oversize plates.

Bauer, P.W., Kelson, K.I., Aby, S.B., Lyman, J., Heynekamp, M., and McCraw, D., 2000, Geologic map of the Ranchos de Taos 7.5-minute quadrangle, Taos County, New Mexico: New Mexico Bureau of Geology and Mineral Resources Open-File Geologic Map 33, scale 1:24,000.

Bauer, P.W., Kelson, K.I., and Aby, S.B., 2005, Geologic map of the Peñasco 7.5-minute quadrangle, Taos County, New Mexico: New Mexico Bureau of Geology and Mineral Resources Open-File Geologic Map 62, scale 1:24,000.

Bauer, P.W., Johnson, P.S., and Timmons, S., 2007, Springs of the Rio Grande Gorge, Taos County, New Mexico: Inventory, Data Report, and Preliminary Geochemistry: New Mexico Bureau of Geology and Mineral Resources Open-File Report 506, 20 p., plus appendices and oversize plate.

Bauer, P.W., Kelson, K.I., Aby, S.B., and Mansell, M.M., 2016, Geologic map of the Picuris Mountains region, Taos County, New Mexico: New Mexico Bureau of Geology & Mineral Resources Open-File Geologic Map, scale 1:24,000, (in review).

Brister, B.S., Bauer, P.W., Read, A.S., and Lueth, V.W., eds., 2004, Geology of the Taos Region: New Mexico Geological Society, 55th Annual Field Conference Guidebook, 448 p.

Chapin, C.E., and Cather, S.M., 1994, Tectonic setting of the axial basins of the northern and central Rio Grande rift, in Keller, G.R. and Cather, S.M., eds., Basins of the Rio Grande Rift: Structure, Stratigraphy and Tectonic Setting: Geological Society of America Special Paper 291, p. 5–25.

Chapin, R.S, 1981, Geology of the Fort Burgwin Ridge, Taos County, New Mexico [M.S. thesis]: Austin, University of Texas, 151 p.

Cordell, L., 1978, Regional geophysical setting of the Rio Grande rift: Geological Society of America Bulletin 89, p. 1073-1090.

Cordell, L., and Keller, G.R., 1984, Regional structural trends inferred from gravity and aeromagnetic data in the New Mexico-Colorado border region, in Baldridge, W.S., Dickerson, P.W., Riecker, R.E., and Zidek, J., eds., Rio Grande Rift, Northern New Mexico: New Mexico Geological Society, 35th Annual Field Conference Guidebook, p. 21-23.

Drakos, P., Lazarus, J., Riesterer, J., White, B., Banet, C., Hodgins, M., and Sandoval, J., 2004a, Subsurface stratigraphy in the southern San Luis Basin, New Mexico; in Brister, B.S., Bauer, P.W., Read, A.S., and Lueth, V.W., eds., Geology of the Taos Region: New Mexico Geological Society, 55th Annual Field Conference Guidebook, p. 374-382.

Drenth, B.J., Bauer, P.W., and Read, Adam S., 2011, Recent gravity studies on Taos Pueblo Lands: Data collection, data processing, and preliminary interpretation: U.S. Geological Survey Administrative Report to Taos Pueblo, April, 2011, 21 p.

Drenth, B.J., Grauch, V.J.S., Thompson, R.A., and Bauer, P.W., 2015, 3D gravity modeling of the San Luis Basin, northern Rio Grande rift, Colorado and New Mexico: Geological Society of America Abstracts with Programs, v. 47, no. 7, p. 741.

Dungan, M.A., Muehlberger, W.R., Leininger, L., Peterson, C., McMillan, N.J., Gunn, G., Lindstrom, M., and Haskin, L., 1984, Volcanic and sedimentary stratigraphy of the Rio Grande gorge and the Late Cenozoic geologic evolution of the southern San Luis Valley, in Baldridge, W.S., Dickerson, P.W., Riecker, R.E., and Zidek, J., eds., Rio Grande Rift Northern New Mexico: New Mexico Geological Society, 35th Annual Field Conference Guidebook, p. 157–170.

Faulds, J.E., and Varga, R.J., 1998, The role of accommodation zones and transfer zones in the regional segmentation of extended terranes: in Faulds, J.E., and Stewart, J.H., eds., Accommodation Zones and Transfer Zones: The Regional Segmentation of the Basin and Range Province: Geological Society of America Special Paper 323, p. 1-45.

Garrabrant, L. A., 1993, Water resources of Taos County, New Mexico: U.S. Geological Survey Water-Resources Investigations Report 93–4107, 86 p.

Glorieta Geoscience, Inc., 2007, Drilling and completion report, Rio Pueblo 3200 feet deep production well (RG-37303-S), Taos, New Mexico: Unpublished technical report prepared for the Town of Taos and Souder, Miller, and Associates, September, 2007, 46 p.

Grauch, V.J.S., and Keller, G.R., 2004, Gravity and aeromagnetic expression of tectonic and volcanic elements of the southern San Luis Basin, New Mexico and Colorado, in Brister, B.S., Bauer, P.W., Read, A.S., and Lueth, V.W., eds., Geology of the Taos Region: New Mexico Geological Society Guidebook, 55th Annual Field Conference Guidebook, p. 230–243.

Grauch, V.J.S., Bauer, P.W., and Kelson, K.I., 2004, Preliminary interpretation of high-resolution aeromagnetic data collected near Taos, New Mexico, in Brister, B.S., Bauer, P.W., Read, A.S., and Lueth, V.W., eds., Geology of the Taos Region: New Mexico Geological Society, 55th Annual Field Conference Guidebook, p. 244-256.

Grauch, V.J.S., Bauer, P.W., Drenth, B.J., and Kelson, K.I., 2015, Making rift connections: Geophysical insights into the geometry and temporal evolution of the Embudo transfer zone and the basin-bounding Sangre de Cristo fault, northern Rio Grande rift, New Mexico: Abstract presented at 2015 Fall Meeting, AGU, San Francisco, California,14-18 December.

Grauch, V.J.S., Bauer, P.W., Drenth, B.J., and Kelson, K.I., 2017, A shifting rift—Geophysical insights into the evolution of Rio Grande rift margins and the Embudo transfer zone near Taos, New Mexico: Geosphere, v. 13 (in press).

Johnson, P.S., Bauer, P.W., and Felix, B., 2016, Hydrogeologic investigation of the southern Taos Valley, Taos County, New Mexico: New Mexico Bureau of Geology and Mineral Resources Open-File Report 581, 95 p.

Kelson, K.I., 1986, Long-term tributary adjustments to base-level lowering in northern Rio Grande rift, New Mexico [M.S. thesis]: Albuquerque, University of New Mexico, 210 p.

Kelson, K.I., and Bauer, P.W., 2003, Geologic map of the Los Cordovas 7.5-minute quadrangle, Taos County, New Mexico: New Mexico Bureau of Geology and Mineral Resources Open-File Geologic Map 63, scale 1:24,000.

Kelson, K.I., Bauer, P.W., and Aby, S.B., 1998, Geology of the Carson 7.5-minute quadrangle, Taos County, New Mexico: New Mexico Bureau of Geology and Mineral Resources Open-File Geologic Map 22, scale 1:24,000.

Kelson, K.I., Bauer, P.W., Connell, S.D., Love, D.W., Rawling, G.C., and Mansell, M.M., 2004b, Initial paleoseismic and hydrogeologic assessment of the southern Sangre de Cristo fault at the Taos Pueblo site, Taos County, New Mexico, in Brister, B.S., Bauer, P.W., Read, A.S., and Lueth, V.W., eds., Geology of the Taos Region: New Mexico Geological Society, 55th Annual Field Conference Guidebook, p. 289-299.

Kelson, K.I., Bauer, P.W., Unruh, J.R., and Bott, J.D.J., 2004a, Late Quaternary characteristics of the northern Embudo fault, Taos County, New Mexico, in Brister, B.S., Bauer, P.W., Read, A.S., and Lueth, V.W., eds., Geology of the Taos Region: New Mexico Geological Society, 55th Annual Field Conference Guidebook, p. 147-157.

Kelson, K.I., Unruh, J.R., and Bott, J.D.J., 1996, Evidence for active rift extension along the Embudo fault, Rio Grande rift, northern New Mexico: Geological Society of America Abstracts with Program, v. 28, no. 7, p. A377.

Kelson, K.I., Unruh, J.R., and Bott, J.D.J., 1997, Field characterization, kinematic analysis, and initial paleoseismic assessment of the Embudo fault, northern New Mexico: Final Technical Report to the U.S. Geological Survey from William Lettis and Associates, Inc., 48 p.

Lambert, P.W., 1966, Notes on the late Cenozoic geology of the Taos-Questa area, New Mexico, in Northrop, S.A., and Read, C.B., eds., Taos-Raton-Spanish Peaks Country (New Mexico and Colorado): New Mexico Geological Society, 17th Annual Field Conference Guidebook, p. 43-50.

Leininger, R.L., 1982, Cenozoic evolution of the southernmost Taos Plateau, New Mexico [M.S. thesis]: Austin, University of Texas, 110 p.

Lipman, P.W., and Mehnert, H.H., 1975, Late Cenozoic basaltic volcanism and development of the Rio Grande depression in the southern Rocky Mountains: Geological Society of America Memoir 144, p. 119–154.

Lipman, P.W., and Mehnert, H.H., 1979, The Taos Plateau volcanic field, northern Rio Grande rift, New Mexico, in Riecker, R.C., ed., Rio Grande rift – Tectonics and magmatism: American Geophysical Union, Washington D.C., p. 289–311.

Lipman, P.W., and Reed, J.C., Jr., 1989, Geologic map of the Latir volcanic field and adjacent areas: U.S. Geological Survey Miscellaneous Investigations Map I-1907, scale 1:48,000.

Machette, M.N., and Personius, S.F., 1984, Quaternary and Pliocene faults in the eastern part of the Aztec quadrangle and the western part of the Raton quadrangle, northern New Mexico: U.S. Geological Survey Map MF-1465-B, scale 1:250,000.

Machette, M.N., Personius, S.F., Kelson, K.I., Haller, K.M., and Dart, R.L., 1998, Map and data for Quaternary faults in New Mexico: U.S. Geological Survey Open-File Report 98-521, 443 p.

Menges, C.M., 1988, The tectonic geomorphology of mountain front landforms in the northern Rio Grande rift, New Mexico [Ph.D. dissertation]: Albuquerque, University of New Mexico, 140 p.

Menges, C.M., 1990, Late Cenozoic rift tectonics and mountain-front landforms of the Sangre de Cristo Mountains near Taos, northern New Mexico, in Bauer, P.W.; Lucas, S.G., Mawer, C.K., and McIntosh, W.C., eds., Tectonic Development of the Southern Sangre de Cristo Mountains, New Mexico: New Mexico Geological Society, 41st Annual Field Conference Guidebook, p. 113-122.

Miller, J.P., Montgomery, A., and Sutherland, P.K., 1963, Geology of part of the Sangre de Cristo Mountains, New Mexico: New Mexico Bureau of Mines and Mineral Resources Memoir 11, 106 p.

Montgomery, A., 1953, Precambrian geology of the Picuris Range, north-central New Mexico: New Mexico Bureau of Mines and Mineral Resources Bulletin 30, 89 p.

Montgomery, A., 1963, Precambrian geology, in Miller, J.P., Montgomery, A., and Sutherland, P.K., Geology of part of the Sangre de Cristo Mountains, New Mexico: New Mexico Bureau of Mines and Mineral Resources Memoir 11, p. 7-21.

Muehlberger, W.R., 1979, The Embudo fault between Pilar and Arroyo Hondo, New Mexico: An active intracontinental transform fault, in, Ingersoll, R.V., Woodward, L.A., James, H.L., eds., Santa Fe Country: New Mexico Geological Society, 30th Annual Field Conference Guidebook, p. 77-82.

Personius, S.F., and Machette, M.N., 1984, Quaternary faulting in the Taos Plateau region, northern New Mexico, in Baldridge, W.S., Dickerson, P.W., Riecker, R.E., and Zidek, J., eds., Rio Grande Rift (Northern New Mexico): New Mexico Geological Society, 30th Annual Field Conference Guidebook, p. 83-90.

Peterson, C.M., 1981, Late Cenozoic stratigraphy and structure of the Taos Plateau, northern New Mexico [M.S. thesis]: Austin, University of Texas, 57 p.

Read, A.S., Thompson, R.A., and Mansell, M.M., 2004, Generalized geologic map of southern San Luis Basin, in Brister, B.S, Bauer, P.W., Read, A.S., and Lueth, V.W., eds., Geology of the Taos Region: New Mexico Geological Society, 55th Annual Field Conference Guidebook, p. 114.

Rehder, T.R., 1986, Stratigraphy, sedimentology, and petrography of the Picuris formation in Ranchos de Taos and Tres Ritos quadrangles, north-central New Mexico [M.S. thesis]: Dallas, Southern Methodist University, 110 p.

Steinpress, M.G., 1980, Neogene stratigraphy and structure of the Dixon area, Espanola basin, north-central New Mexico [M.S. thesis]: Albuquerque, University of New Mexico, 127 p.

Thompson, R.A., and Machette, M.N., 1989, Geologic Map of the San Luis Hills Area, Conejos and Costilla Counties, Colorado: U.S. Geological Survey Miscellaneous Investigations Series Map I–1906, scale 1:50,000.

Thompson, R.A., Johnson, C.M., and Mehnert, H. H., 1991, Oligocene basaltic volcanism of the north Rio Grande rift: San Luis Hills, Colorado: Journal of Geophysical Research, v. 96, p. 13,577–13,592.

Wells, S.G., Kelson, K.I., and Menges, C. M., 1987, Quaternary evolution of fluvial systems in the northern Rio Grande rift, New Mexico and Colorado: Implications for entrenchment and integration of drainage systems, in Menges, C., Enzel, Y., and Harrison, B., eds., Quaternary tectonics, landform evolution, soil chronologies and glacial deposits—Northern Rio Grande rift of New Mexico: Friends of the Pleistocene, Rocky Mountain Cell, Guidebook, p. 55-69.

# APPENDIX 1
# Description of map units for geologic map and cross sections (plates 1 & 2) of the southern Taos Valley study area.

by Paul W. Bauer, Keith I. Kelson, and Scott B. Aby
January, 2016

## CENOZOIC DEPOSITS AND ROCKS

**af** **Artificial fill and disturbed land** (modern-historic)—Excavations and areas of human-deposited fill and debris; shown only where aerially extensive

**Qal** **Alluvium** (latest Pleistocene and Holocene)—Generally brownish and/or reddish, poorly to moderately sorted, angular to rounded, thinly to thickly bedded, loose silt and silty sand with subordinate coarse lenses and thin to medium beds of mostly locally derived clasts; mapped in active channels, floodplains, low (young) alluvial terraces, tributary-mouth fans, and some valley-slope colluvial deposits; weak to no soil development; piece of charcoal from within Qal yielded conventional 14C ages ranging from about 3275 to 1800 yrs before present; up to 7 m estimated thickness

**Qe** **Eolian deposits** (late Pleistocene to Holocene)—Light-colored, well-sorted, fine to medium sand and silt deposits that are recognized as laterally extensive, low-relief, sparsely vegetated, mostly inactive, sand dunes and sand sheets that overlie Servilleta Basalt on the Taos Plateau; rare gravel lag; weak to moderate soil development; northeast-trending longitudinal dune-crest orientations; predominant wind direction from southwest; up to several meters thick

**Qc** **Colluvium** (middle Pleistocene to Holocene)—Mostly locally derived, light- to dark-brown, orange, and rarely reddish, poorly to moderately sorted, angular to well-rounded, silty to sandy conglomerate/breccia with clasts locally to >1m; mapped on hill slopes and valley margins only where it obscures underlying relations; estimated at generally less than 5 m thick

**Qls** **Landslides in Rio Grande gorge and tributaries** (late Pleistocene to Holocene)—Poorly sorted rock debris and sand to boulder debris transported downslope; occurs on slopes marked by hummocky topography and downslope-facing scarps; includes small earth flow, block-slump, and block-slide deposits; includes large rotational Toreva slide blocks within the Rio Grande and Rio Pueblo de Taos gorges, which include large, rotated and detached blocks of intact Servilleta Basalt; south of the Rio Grande, landslide deposits do not form well-defined lobes, as they do to the north, and may be partly colluvial; the southern deposits are poorly exposed except in road cuts along the highway just north of Rinconada where the deposits are arranged in thick, apparently tabular bodies with a range of compositions

**Qac/Tp** **Alluvial and colluvial deposits** (Holocene to Pleistocene)—Poorly exposed gravel and sand composed of Tertiary volcanic clasts and/or granitic clasts and gruss; overlies Tpl and Tpt-Ttc in complexly faulted area in Miranda Canyon; approximately 5-10(?) m thick

**Qfy Qty** **Young alluvial-fan and stream terrace deposits** (latest Pleistocene to Holocene)—Poorly sorted deposits of silt, sand, pebbles, cobbles and boulders; deposits are typically clast-supported and poorly bedded; pebble and cobble clasts are typically imbricated; terrace deposits unconformably overlie the

local bedrock; clasts are primarily sedimentary rocks, quartzite, slate, schist, metavolcanic, granitic rocks, and Tertiary granitic and volcanic rocks; uppermost sediments are commonly silty sand, probably overbank deposits; weak to moderate pedogenic development, including A, Bw, Bwk and Bk soil horizons and stage I to II calcium carbonate development; map unit Qty is typically on valley floors of large to medium drainages, whereas Qfy exists as young mountain-front fans and valley fills in small tributaries; thickness up to 5 m

**Qt6rp Stream terrace deposits of the Rio Pueblo de Taos and tributaries** (latest Pleistocene)—Poorly sorted silt, sand, pebbles, cobbles, and boulders; clasts primarily of quartzite, schist, granite, and volcanic rock types; associated soils have stage I to II calcium carbonate development; typically present as thin (< 5 m) alluvial deposit on strath surface cut on volcanic bedrock or unit QTL; associated with the Q6 surface of Kelson (1986)

**Qf4 Qt4rp Alluvial-fan and stream terrace deposits of the Rio Pueblo de Taos and tributaries** (middle? to late Pleistocene)—Poorly sorted silt, sand, pebbles, and boulders; associated soils have stage III calcium carbonate development, argillic Bt soil horizons and 10YR to 7.5YR hues in Bt horizons; clasts primarily of granitic and metamorphic rocks north of Rio Pueblo de Taos, and granitic, metamorphic, and sedimentary rock types south of Rio Pueblo de Taos; clasts also include basaltic rock types along Arroyo Seco and along Rio Pueblo de Taos downstream of Los Cordovas; modified from Kelson (1986)

**Qf3 Qt3rp Alluvial-fan and stream terrace deposits of the Rio Pueblo de Taos and tributaries** (middle to late Pleistocene)—Poorly sorted silt, sand, pebbles, and boulders; stage II to III calcium carbonate development; clasts primarily of quartzite, slate, and schist; granitic clasts also exist east of Arroyo del Alamo

**Qf2 Qt2rp Alluvial-fan and stream terrace deposits of the Rio Pueblo de Taos and tributaries** (middle? Pleistocene)—Poorly sorted silt, sand, pebbles, and boulders; clasts primarily of granitic and metamorphic rocks north of Rio Pueblo de Taos, and granitic, metamorphic and sedimentary rocks south of Rio Pueblo de Taos; associated soils have stage III to IV calcium carbonate development, thick argillic Bt soil horizons, and 7.5YR to 10YR hues in soil Bt horizons; upper soil horizons may be affected by surface erosion; modified from Kelson (1986); finer grained to the north, away from the Picuris Mountains range front; grouped into unit Qfo northeast of the Rio Grande del Rancho

**Qt2rg Stream terrace deposits of the Rio Grande** (middle? Pleistocene)—Poorly sorted silt, sand, pebbles, and boulders; clasts primarily of granitic, metamorphic, intermediate volcanic, basalt, and sedimentary rocks; locally may contain clasts of Tertiary Amalia Tuff; associated soils have stage III to IV calcium carbonate development, thick argillic Bt soil horizons, and 7.5YR to 10YR hues in soil Bt horizons; upper soil horizons may be affected by surface erosion; may be mantled locally by unit Qe; modified from Kelson (1986); estimated thickness 1 to 10 m

**Qf1 Qt1rp Alluvial-fan and stream terrace deposits of the Rio Pueblo de Taos and tributaries** (middle Pleistocene)—Poorly sorted silt, sand, pebbles, and boulders; clasts primarily of quartzite, slate, and schist; granitic clasts also present east of Arroyo del Alamo; finer grained to the north, away from the Picuris Mountains range front; stage III to IV calcium carbonate development, although soil horizons are commonly affected by surface erosion; Qf1 is differentiated from QTL by larger clast size (Kelson, 1986), less oxidation, poor sorting, absence of abundant manganese oxide staining, and clasts that are less weathered; ash probably within Qf1 deposits at locality near Stakeout Road dated at 1.27 ± 0.02 Ma (40Ar-39Ar method, W. McIntosh, personal communication, 1996); where exposed to the south, thickness is up to 12 m

**Qfu Alluvial fan deposits, undivided** (middle to late Pleistocene)—Poorly sorted silt, sand, pebbles, and cobbles; mapped along majority of Sangre de Cristo range front, but not correlated to other fan units because of lack of well-defined age control, clear stratigraphic position, or distinct lithologic characteristics; probably correlative with alluvial fan deposits Qf1 through Qf6; shown on map as Qfu/QTL where a thin layer of Qfu overlies QTL

**Qfo Qto Alluvial fan and terrace deposits, undivided** (middle to late Pleistocene)—Poorly sorted deposits of silt, sand, and pebbles; deposits are typically matrix-supported and poorly bedded; clasts are primarily Paleozoic sedimentary rocks and Proterozoic granitic and metamorphic rock types; on Pilar Mesa, deposit

is dominated by slate pebbles and cobbles; between Arroyo del Alamo and Arroyo Hondo, deposit commonly is gravel remnants preserved on interfluves; moderate pedogenic development, including A, Bt, Btk and Bk soil horizons and stage III and IV calcium carbonate development; upper soil horizons are commonly affected by surface erosion; map unit Qto typically occurs as isolated remnants on ridge crests, and is probably correlative with units Qt1 through Qt4, whereas Qfo exists as mountain-front fans and probably overlaps with units Qf2 through Qf4, but not assigned to other fan units because of lack of well-defined age control, clear stratigraphic position, and distinct lithologic characteristics; thickness up to 3 m

**Tsb** **Servilleta Basalt** (Pliocene)—Tsb can locally be subdivided into lower Servilleta Basalt (Tsbl), middle Servilleta Basalt (Tsbm), and upper Servilleta Basalt (Tsbu) (Dungan et al., 1984); flows of dark-gray tholeiitic basalt characterized by small olivine and tabular plagioclase phenocrysts, diktytaxitic texture, and local vesicle pipes and segregation veins; forms thin, fluid, widespread pahoehoe basalt flows of the Taos Plateau volcanic field erupted principally from large shield volcanoes in the central part of the Taos Plateau (Lipman and Mehnert, 1979) but also from several small shields and vents to the northwest of the map area near the Colorado border (Thompson and Machette, 1989; K. Turner, personal communication, 2014); additional buried vents west of the Rio Grande are likely; flows typically form columnar-jointed cliffs where exposed, with a maximum thickness of approximately 50 m in the Rio Grande gorge approximately 16 km northwest of Taos; separated by sedimentary intervals as much as 70 m thick in the southern part of the map area (Leininger, 1982); 40Ar/39Ar ages from basalts exposed in the Rio Grande gorge (Cosca et al., 2014) range in age from 4.78 +/- 0.03 Ma for the lowest basalt near the Gorge Bridge, to 3.59 +/- 0.08 Ma for the highest basalt flow at the Gorge Bridge, broadly consistent with previous results by Appelt (1998); the base of the upper Servilleta Basalt lava flow section at La Junta Point yielded an 40Ar/39Ar age of 3.78 +/- 0.08 Ma (sample 10RG05 - M. Cosca, personal communication, 2014), whereas a lava flow at the base of the section south of Cerro Chiflo yielded an 40Ar/39Ar age of 3.78 +/- 0.08 Ma (sample RT08GM02 - M. Cosca, personal communication, 2014)

**QTL** **Lama formation** (Pliocene to early? Pleistocene)—Poorly sorted sand, pebbles, and cobbles; clasts of basalt, quartzite, other metamorphic rock types, and other volcanic rock types; locally high percentage of angular to subangular quartzite pebbles and cobbles; commonly cross-bedded, and stained with black manganese oxide and yellowish-orange iron oxide coatings; oxidized; clasts are typically weathered or grussified; contains distinct discontinuous sandy interbeds; commonly crudely imbricated; imbrication suggests westerly flow direction in area north of Taos Municipal Airport, and southerly flow direction in areas north and west of Rio Pueblo de Taos, with northwesterly flow direction in area southeast of Rio Pueblo de Taos; well drillers records in the Questa area show clay layers in the shallow subsurface that are interpreted as lacustrine deposits; the unit is present between the Sangre de Cristo Mountains range front and the Rio Grande gorge over most of the map area; correlative with Lambert's (1966) two informal facies of the "Servilleta Formation" (the "sandy gravel facies" found south of the Rio Hondo, and the "gravelly silt facies" found between the Rio Hondo and the Red River); correlative with Kelson's (1986) informal "Basin Fill deposit;" correlative with the unit previously informally called "Blueberry Hill formation" in the Taos area; also correlative with Pazzaglia's (1989) late Neogene-Quaternary rift fill sequence (unit Q1) which he informally named the Lama formation; herein, for this study area, the Lama formation is defined as the uppermost, pre-incision, sedimentary rift fill, and where extant represents the uppermost member of the Santa Fe Group; the unit therefore includes all of the basin fill between the oldest Servilleta Basalt (5.55 +/- 0.37 Ma near Cerro Azul, D. Koning, personal communication, 2015) and the oldest Rio Grande (and tributary) terrace gravels (e.g., Qt0rg, Qt0rr); the Lama formation and the underlying Chamita Formation are texturally and compositionally similar and may be indistinguishable in boreholes, although Koning et al. (2015) noted a coarsening of sediment (southwest of the map area) that roughly coincides with the Chamita/Lama contact in the map area; the top of the Lama formation is typically marked by a sharp unconformity and color/textural contrasts with overlying gravels; the unit contains several laterally variable components of sedimentary fill that are associated with various provenance areas related to east- or west-flowing tributary watersheds that have been fairly persistent in the late Cenozoic; locally contains tephra layers; reworked tephra in a road cut near the Red River Fish Hatchery (elevation ca. 7160 ft) was probably derived from nearby ca. 5 Ma volcanic units (R. Thompson, personal

communication, 2015); a tephra in the uppermost Lama formation yielded a date of ~1.6 Ma based on a chemical correlation with the 1.61 Ma Guaje Pumice eruption in the Jemez Mountains (elevation ca. 7660 ft, M. Machette, USGS, personal communication, 2008); thickness ranges from zero to an exposed thickness of about 25 m at the southwestern end of Blueberry Hill, but may be considerably thicker in other parts of the map area

**Tlc** **Clay, Lama formation** (Pliocene)—In cross sections only. Light gray, sedimentary clay layer that is poorly exposed in the walls of the Rio Grande gorge; small (20 to 50 microns) crystals in clay matrix are composed of quartz and feldspar (both plutonic and volcanic); relatively uniform grain size; lies within the clastic units of the Lama formation; where exposed, spatially related to small springs and seeps that are exposed on the nearby canyon walls at elevations of approximately 6200 ft; locally exposed to the southwest near the Village of Pilar where springs emerge along the top of the layer at elevations of about 6300 ft; could be an eolian layer, but more likely a lacustrine clay that accumulated behind a basalt-dammed ancestral Rio Grande; thickness is estimated at 1 to 3 m

**Tc** **Chamita Formation, undivided, Santa Fe Group** (Miocene? and Pliocene)—In cross sections only. Sedimentary deposits between the lowest Servilleta Basalt and the Tesuque Formation; typically rounded to subrounded pebble- to cobble-size clasts in a sand to silt matrix; thick sections to the south reflect Proterozoic clast provenance and are dominated by schist, quartzite, and amphibolite with lesser volcanic clasts derived from the Latir volcanic field; locally, thin interbeds are typically dominated by pebble-size clasts in a fine sand to silt matrix and commonly includes the rock types above in addition to subangular and subrounded volcanic clasts derived locally from adjacent volcanic highlands of the Taos Plateau volcanic field; the top of Tc is herein defined as the sediments below the youngest Servilleta Basalt flows

**Tto** **Ojo Caliente Sandstone of Tesuque Formation, Santa Fe Group** (Miocene)—Very pale brown (10 YR7/4), well- to moderately well-sorted, subrounded to rounded, loose to moderately well indurated sandstone; this unit is a distinctive eolian sand dune deposit sourced from the southwest (Galusha and Blick, 1971); dominant grain size is fine sand; abundant 1.3-5.0 cm thick, brown, CaCO3 concretions; QFL proportions near Dixon average 62% quartz, 28% feldspar, 10% lithics and LvLsLm ratio averages 82% Lv, 8% Ls, and 10% Lm (Steinpress, 1980); thin reddish-brown, finely laminated siltstone horizons exist locally; tabular crossbeds are common, with sets over 4 m in height; the best exposures are in roadcuts along NM-68, northeast of Pilar; in the map area, these sediments underlie the Pilar Mesa member of the Chamita Formation below an interfingering(?) contact, and some of the sand in the Pilar Mesa member is probably reworked Ojo Caliente Sandstone and/or sand derived from the same source during Pilar Mesa member time; age range of 13.5-10.9 Ma is based on regional relationships (Koning et al., 2005); approximately 250 m thick

**Ttc** **Chama-El Rito Member of Tesuque Formation, Santa Fe Group** (Miocene)—Buff, whitish, pink, red and brownish, moderately to very poorly sorted, subangular to subrounded, tabular to lensoidal(?), thinly to very thickly bedded, massive, plane-bedded, or crossbedded, loose to carbonate-cemented muddy siltstone to silty, very fine to very coarse sandstone interbedded with moderately to poorly sorted, mostly subrounded, medium- to very thick-bedded tabular beds and broad lenses of silty/sandy and sandy pebble conglomerate; clasts composed mostly of Tertiary volcanic rocks and quartzite with lesser amounts of Paleozoic sandstone, granitic rocks, Pilar Formation slate, schist, and rare amphibolite; ranges in age regionally from possibly >22 Ma to ~13 Ma (Aby, 2008); thickness unknown, but is expected to range considerably in the subsurface

**Tpt-Ttc** **Tuffaceous member of Picuris Formation and/or Chama-El Rito Member of Tesuque Formation, undivided** (Miocene)—Interbedded and/or complexly faulted, poorly exposed, sparse outcrops of tuffaceous and pumiceous silty sandstones and volcaniclastic sandstone and conglomerate; stratigraphic/temporal relations between the tuffaceous members of the Picuris Formation and the Chama-El Rito Member are discernible (and clearly 'layer cake') in the southern Picuris Mountains, however, locally the Tuffaceous member is either absent or not exposed along most of the range front; along the northeastern edge of the map area are poorly exposed, and possibly complexly faulted, outcrops of both tuffaceous and volcaniclastic rocks that indicate possible interfingering of the two units; elsewhere, these rocks were referred to as the middle tuffaceous member of the Picuris Formation (Aby et al., 2004); age is less than

~25 Ma based on abundant clasts of 25 Ma Amalia Tuff, but minimum age is unknown; thickness in the map area is unknown

**Tp** **Picuris Formation, undivided** (Oligocene to Miocene)- In cross section only. In the Picuris Mountains area (Aby et al., 2004) consists of an upper member of tuffaceous and pumiceous silty sandstones and volcaniclastic sandstone and conglomerate; a member of buff to white and/or pinkish, silty sandstone to fine cobble conglomerate and nonfriable to strong, very fine lower to very coarse upper, very poorly to moderately sorted, rounded to subangular, thinly to thickly bedded, silica-cemented silty to pebbly sandstone which locally contains a basal portion of poorly sorted pebbly/gravelly sandstone and/or cobble/boulder conglomerate composed exclusively of Proterozoic clasts; a member of light buff, yellowish, and locally white, ash-rich, quartzose, silty, fine sand to pebbly, pumiceous sandstone; a lower member of red, greenish, and yellowish, moderately to very poorly sorted, subangular to subrounded, pebbly/silty sandstone and mudstone containing very thick(?) to thin beds and/or lenses and/or isolated clasts of subangular to rounded Proterozoic quartzite (up to 3 m across) and massive quartzite conglomerate; paleoflow measurements indicate source to the north (Rehder, 1986); age range is from at least 35.6 Ma to less than 25 Ma; thickness unknown, but at least 450 m in the Picuris Mountains area

**Tplq** **Llano Quemado Breccia member of Picuris Formation** (Oligocene)—Light gray to red, monolithologic volcanic breccia of distinctive extremely angular, poorly sorted, light-gray, recrystallized rhyolite clasts in a generally reddish matrix; rhyolite clasts contain phenocrysts of biotite, sanidine, and quartz; highly lithified, due to partial welding of the matrix rather than silica or carbonate cement; ridge-former; unit shows both clast and matrix support; beds are generally 1-8 m thick; clasts are up to 15 cm in diameter, and overall clast size decreases southward; less than 1% of clasts are Proterozoic slate and weathered Tertiary volcanic rocks; the breccia is interpreted as a series of flows from a now-buried, nearby rhyolite vent (Rehder, 1986); 40Ar/39Ar date on sanidine from a rhyolite clast collected 1 km southwest of Ponce de Leon spring is 28.35 ± 0.11 Ma; apparent thicknesses of 5-45 m, although subsurface extent is unknown

**Tpa** **Andesitic porphyry** (Oligocene)—Poorly exposed, reddish-gray, andesitic porphyry that is exposed only in a single small exposure in northern Miranda Canyon where it appears to underlie Tplq; age unknown, although it may be related to the volcanic component of Tplq

**Tpl** **Lower member of Picuris Formation** (Oligocene)—Mostly poorly exposed, red, greenish, and yellowish, moderately to very poorly sorted, subangular to subrounded, pebbly/silty sandstone and mudstone containing very thick(?) to thin beds and/or lenses and/or isolated clasts of subangular to rounded Proterozoic quartzite (up to 3 m across) and massive quartzite conglomerate; commonly highly weathered with fractured clasts; most available exposures consist of very well-carbonate-cemented quartzite pebble and cobble conglomerate intervals exposed near mapped faults; the lower contact is placed at the first accumulation of diverse Proterozoic clasts (quartzite, Pilar Formation slate, +/-schist); the upper 10 m in Agua Caliente Canyon is a well-exposed bed of well-sorted, quartzite-cobble conglomerate (figure 7 of Aby et al., 2004); the orientation of 95 well-imbricated clasts in this interval suggest derivation from the northeast (average paleotransport direction =143 degrees), at odds with a previous interpretation that this unit was derived from the Picuris Mountains to the southeast (Leininger, 1982); this unit was informally named the Bradley Conglomerate member of the Tesuque Formation (Leininger, 1982), but that name has been abandoned; this unit has also been referred to as the Lower Conglomerate member of the Picuris Formation (Aby et al., 2004) but, locally, much of the unit is fine grained; near the top(?) of the section in Agua Caliente Canyon is an ash layer dated at 34.5 ± 1.2 Ma by 40Ar/39Ar (Aby et al., 2004); regionally, this unit contains variable amounts of intermediate composition volcanic rocks (dated by 40Ar/39Ar at 32.4 to 28.8 Ma; Aby et al., 2007), and fluvially reworked Llano Quemado breccia (28.35 Ma); the oldest ashes are dated at 35.5 Ma and 35.6 Ma (Aby et al., 2004), but maximum age of unit is unknown; at least 250 m thick where not faulted

**Tbo** **Older basaltic rocks** (Oligocene)—In cross section only. Volcanic rocks that predate the Tesuque Formation and may exist within the Picuris Formation; may include the Hinsdale Formation and/or similar units; thickness unknown, but probably less than 30 m

## PALEOZOIC ROCKS

**breccia** **Mixed fault breccia** (late Proterozoic? to Tertiary?)—Fault breccia composed of a mixture of Paleoproterozoic Hondo Group, Vadito Group, and granitic rock along the Picuris-Pecos fault; ridge former where the breccia is strongly silicified

**ℙ, ℙu** **Sedimentary rocks of the Taos Trough, undivided** (Pennsylvanian)—Poorly exposed; greenish, reddish, yellowish, buff, tan, black, and brown; very friable-to-firm; sandy to clayey; thinly to thickly bedded; poorly to moderately well-cemented(?), sandy to clayey siltstone, mudstone, and shale interbedded with mostly greenish and brownish, firm to very strong, poorly to moderately well-sorted, poorly to moderately well rounded, thin- to very thickly bedded, moderately to very well-cemented, quartzose, feldspathic, and arkosic, silty to pebbly sandstone and sandy conglomerate and less common thin- to thick-bedded, grayish and blackish limestone of the Alamitos and Flechado Formations; contains a rich assortment of fossils; sandstones commonly contain plant fragments that have been altered to limonite(?); contacts between beds are generally sharp, rarely with minor scour (less than ~20 cm); the lower contact is sharp, planar(?), and disconformable(?) where it overlies Mississippian rocks; lower contact is mapped at the top of the Del Padre Sandstone or highest Mississippian carbonate, or at the base of the lowest sedimentary bed where Mississippian rocks are absent; conglomeratic layers in the lower part of the unit locally contain rare, sometimes banded, chert pebbles; equivalent to the Sandia, Madera, and La Posado Formations to the south; colluvial deposits have not been mapped on the Tres Ritos quadrangle, but most of the Pennsylvanian rocks are covered by brown to nearly black, loose, very poorly sorted, rounded to angular, massive- to very crudely bedded, sandy-silty conglomerate and pebbly silty sand; this material is clearly colluvial based on its landscape position and the random orientation of larger clasts within a matrix of usually dark, organic-rich fines; windthrow (movement of soil by toppling of trees) is thought to be an active process in the map area, and is probably responsible for the pervasive colluvial mantle; fusilinids collected in the Taos quadrangle are Desmoinesian in age (Bruce Allen, personal communication, 2000); Miller et al. (1963) measured an incomplete section of 1756 m along the Rio Pueblo near the Comales Campground, and an aggregate thickness of Pennsylvanian strata in the map area of >1830 m

**Mu** **Sedimentary rocks of the Arroyo Penasco Group** (Mississippian)—Includes the Del Padre Sandstone member of Espiritu Santa Formation, the Espiritu Santa Formation carbonate sedimentary rocks, and the Tererro Formation carbonate sedimentary rocks

## PROTEROZOIC ROCKS OF THE PICURIS MOUNTAINS

**Ytpl** **Piedra Lumbre Formation, Trampas Group** (Mesoproterozoic)—Includes several distinctive rock types: 1) quartz-muscovite-biotite-garnet-staurolite phyllitic schist with characteristic sheen on crenulated cleavage surfaces; euhedral garnets are 1 mm, biotite books are 2 mm, and scattered anhedral staurolites are up to 5 mm in diameter; 2) finely laminated light gray phyllitic quartz-muscovite-biotite-garnet schist and darker bluish gray fine-grained biotite quartzite to metasiltstone; quartzite layers range in thickness from 1 cm to 1 m; and 3) light-gray to gray garnet schist with lenses of quartzite to metasiltstone; calc-silicate layers exist locally; original sedimentary structures including graded bedding are preserved; well-developed cleavage parallel to both layering and axial surfaces of small intrafolial isoclinal folds; dominant layering in much of this unit is transpositional; in the core of the Hondo syncline, unit is thicker, contains a greater variety of rock types, and is gradational with the Pilar Formation; U-Pb analyses of detrital zircons from a quartzite in the upper part of the section (unit Ytplq?) were interpreted to constrain the unit to be less than about 1470 Ma in depositional age (Daniel et al., 2013); apparent thickness is 200-400 m

**Ytp** **Pilar Formation, Trampas Group** (Mesoproterozoic)—Dark gray to black, carbonaceous phyllitic slate; extremely fine-grained homogeneous rock except for rare 1- to 2-cm-thick light-colored bands of quartz and muscovite that may represent original sedimentary bedding; in thin section, fine-grained matrix

consists of quartz (50-70%), muscovite (15-30%), and prominent streaky areas of graphitic material; lenticular porphyroblasts (0.1 to 0.5 mm) are altered to yellow-brown limonite; pervasive slaty cleavage is locally crenulated; small isoclinal folds locally; basal 1.5-m-thick, black to blue-black, medium-grained, garnet quartzite is distinctive; garnets are anhedral, oxidized, and red-weathered; gradational with Ytpl; Daniel et al. (2013) calculated a mean 207Pb/206Pb zircon age of 1488 ± 6 Ma for a 1-2-m-thick, white, schistose layer that was interpreted as a metamorphosed tuff, and therefore represents the depositional age of the sedimentary protolith; thickness unknown due to extreme ductile deformation

**Xpeg** **Pegmatite** (Mesoproterozoic)—Includes both simple (quartz-K-feldspar-plagioclase-muscovite) pegmatites and complex zoned pegmatites containing rare minerals in the Trampas quadrangle; simple pegmatites are by far the most abundant in the map area; pegmatite bodies typically are dikes or lenses, locally aligned parallel to country rock foliation; thicknesses range from 2 cm to 15 m; no apparent spatial relationship exists between pegmatite bodies and plutonic bodies, and no evidence exists to suggest that pegmatites are connected to plutons at depth; more than one generation of pegmatite formation is represented, and at least one generation is younger than the youngest granite at 1450 Ma (Long, 1976)

**Xh** **Hondo Group, undivided** (Paleoproterozoic)—In cross section only. Schist and quartzite units of the Ortega and Rinconada Formations

**Xhr** **Rinconada Formation, undivided** (Paleoproterozoic)—Undivided schists and quartzites near the Pilar-Vadito fault in the Carson quadrangle that are pervasively fractured and faulted; U-Pb analyses of detrital zircons from two quartzite units was interpreted to constrain the unit to be less than about 1700 Ma in depositional age (Daniel et al., 2013)

**Xhr6** **R6 schist member, Rinconada Formation** (Paleoproterozoic)—Tan, gray, silver quartz-muscovite-biotite-staurolite-garnet schistose phyllite interlayered with fine-grained, garnet-bearing, muscovite quartzite; euhedral staurolites (<5 cm) abundant in some layers; small euhedral garnets (<2 mm) throughout; strong parting along well-developed foliation; sharp contact with Ytp might represent a large unconformity; thickness is approximately 90 m

**Xhr5** **R5 quartzite member, Rinconada Formation** (Paleoproterozoic)—Variety of white to blue medium-grained quartzites interlayered with fine-grained schistose quartzites and quartzose schists; measured section by Hall (1988) from top to bottom: 1) tan to white, friable, thinly layered, crossbedded micaceous quartzite; 2) blue, medium-grained, thickly layered, resistant saccharoidal quartzite; locally crossbedded; 3) white to tan, friable schistose quartzite layered with blue, medium-grained saccharoidal quartzite; thin layers of fine-grained quartz-muscovite-biotite schist; basal 1.5 m massive blue medium-grained quartzite; 4) tan, thinly layered, micaceous quartzite layered with quartz-rich muscovite schist; abundant crossbedding; 5) blue and white streaked, thickly bedded, medium-grained quartzite with abundant crossbedding; and 6) tan, thinly layered, micaceous quartzite interlayered with quartz-rich quartz-muscovite schist; abundant crossbedding; gradational contact with Xhr6; thickness is approximately 75 m

**Xhr3** **R3 quartzite member, Rinconada Formation** (Paleoproterozoic)—Interlayered crossbedded quartzites and pelitic schists; distinctive marker layer near center of unit is 25-m-thick, white, thinly bedded, ridge-forming quartzite; sharp contact with Xhr4; thickness is approximately 75 m

**Xhr1/2** **R1/R2 schist member, Rinconada Formation** (Paleoproterozoic)—Lower unit of fine- to medium-grained, tan to silver, quartz-muscovite-biotite schist with small euhedral garnets (<2mm) and scattered euhedral staurolite twins (<1.5cm); near base are black biotite books (<2cm) and on the upright limb of the Hondo syncline in Section 7 are spectacular, andalusite porphyroblasts up to 8 cm across; upper unit of gray to tan, red-weathering, coarse-grained quartz-muscovite-biotite-staurolite-albite-garnet schist containing interlayers of 1-10 cm, red-, gray-, or tan-weathering, fine-grained, muscovite-garnet quartzite; abundant staurolites are twinned, euhedral, up to 3 cm; abundant garnets are euhedral and small (<2mm); strong parting along foliation plane; sharp to gradational contact with Xhr3; lower and upper unit have previously been subdivided into R1 and R2 members, respectively, based on mineralogy (Nielsen, 1972); thickness is approximately 265 m

**Xho** **Ortega Formation, Hondo Group, undivided** (Paleoproterozoic)—Gray to grayish-white, medium- to coarse-grained quartzite; generally massive and highly resistant to weathering; locally well-cross-bedded,

with kyanite- or sillimanite-concentrated in thin, schistose, muscovite-rich horizons; crossbeds are defined by concentrations of black iron-oxide minerals; common accessory minerals are ilmenite, hematite, tourmaline, epidote, muscovite, and zircon; gradational contact with Rinconada Formation; U-Pb analyses of detrital zircons from two quartzite layers was interpreted to constrain the unit to be less than about 1700 Ma in depositional age (Daniel et al., 2013); thickness is 800-1200 m

**Xmg** **Miranda granite** (Paleoproterozoic?)—East of the Picuris-Pecos fault; typically consists of pink to white, medium-grained, mica-rich, granitic rock with euhedral megacrysts of feldspar; these granitic rocks are everywhere weathered looking, fairly equigranular, and commonly crumbly; appears to intrude the Rio Pueblo schist along its southern contact; pegmatites are locally voluminous; contains at least one tectonic foliation; three closely spaced, orthogonal joint sets cause this rock to weather into small, angular blocks; age unknown, but similar in occurrence and texture to the ca. 1.6 Ga Tres Piedras Granite of the east-central Tusas Mountains

**Xvg** **Glenwoody Formation** (Paleoproterozoic)—Feldspathic quartz-muscovite schist and quartzose schist exposed in isolated exposures along the northern flank of the Picuris Mountains and in the Pilar cliffs; white, light gray, pink, or green; commonly contains megacrysts of feldspar and rounded and flattened quartz in a fine-grained matrix of quartz, muscovite and feldspar; contact with overlying Ortega Formation is a south-dipping ductile shear zone; pervasive extension lineation in schist plunges south; upper 40 m of schist is pinkish, and contains anomalous manganese and rare earth elements, and unusual minerals such as piemontite, thulite, and Mn-andalusite (viridine); L.T. Silver reported a preliminary U-Pb zircon age of ca. 1700 Ma (Bauer and Pollock, 1993); may be equivalent to the Rio Pueblo schist and the ca. 1700 Ma Burned Mountain Formation of the Tusas Mountains; base unexposed; minimum thickness is about 200 m

**Xv** **Vadito Group, undivided** (Paleoproterozoic)—Metavolcanic, metavolcaniclastic, and metasedimentary rocks; U-Pb analyses of detrital zircons from a a schist and a conglomerate layer was interpreted to constrain the unit to be less than about 1700 Ma in depositional age (Daniel et al., 2013)

**XYu** **Proterozoic rocks, undivided** (Paleoproterozoic and Mesoproterozoic)—In cross section only. Supracrustal metamorphic rocks, metaplutonic rocks, and plutonic rocks

## References Cited


Aby, S.B., 2008, Geologic Map of the Servilleta Plaza quadrangle, Taos County, New Mexico: New Mexico Bureau of Geology and Mineral Resources Open-File Geologic Map OF-GM 182, scale 1:24,000.

Aby, S.B., Hallet, B., and Bauer, P.W., 2007, Geologic map of the Tres Ritos quadrangle, Taos County, New Mexico: New Mexico Bureau of Geology and Mineral Resources Open-File Geologic Map OF-GM 145, scale 1:24,000.

Aby. S.B., Bauer, P.W., and Kelson, K.I., 2004, The Picuris Formation: A late Eocene to Miocene sedimentary sequence in northern New Mexico, in Brister, B.S, Bauer, P.W., Read, A.S., and Lueth, V.W., eds., Geology of the Taos Region: New Mexico Geological Society, 55th Annual Field Conference, p. 335-350.

Appelt, R.M., 1998, 40Ar/39Ar geochronology and volcanic evolution of the Taos Plateau volcanic field, northern New Mexico and southern Colorado [M.S. thesis]: Socorro, New Mexico Institute of Mining and Technology, 58 p.

Bauer, P.W., and Pollock, T.R., 1993, Compilation of Precambrian Isotopic Ages in New Mexico: New Mexico Bureau of Geology and Mineral Resources Open-File Report 389, 130 p.

Cosca, M., Thompson, R., and Turner, K., 2014, High precision 40Ar/39Ar geochronology of Servilleta Basalts of the Rio Grande gorge, New Mexico: Abstract V51A-4728 presented at 2014 Fall Meeting, AGU, San Francisco, California, 15-19 December.

Daniel, C.G., Pfeifer, L.S., Jones III, J.V., and McFarlane, C.M., 2013, Detrital zircon evidence for non-Laurentian provenance, Mesoproterozoic (ca. 1490-1450) deposition and orogenesis in a reconstructed orogenic belt, northern New Mexico, USA: Defining the Picuris orogeny: Geological Society of America Bulletin, v. 125, no. 9/10, p. 1423-1441.

Dungan, M.A., Muehlberger, W.R., Leininger, L., Peterson, C., McMillan, N.J., Gunn, G., Lindstrom, M., and Haskin, L., 1984, Volcanic and sedimentary stratigraphy of the Rio Grande Gorge and the Late Cenozoic geologic evolution of the southern San Luis Valley: in Baldridge, W.S., Dickerson, P.W., Riecker, R.E., and Zidek, J., Rio Grande Rift (Northern New Mexico): New Mexico Geological Society, 35th Annual Field Conference, Guidebook, p. 157–170.

Galusha, T., and Blick, J.C., 1971, Stratigraphy of the Santa Fe Group, New Mexico: American Museum of Natural History Bulletin 144, 127 p.

Kelson, K.I., 1986, Long-term tributary adjustments to base level lowering in northern Rio Grande rift, New Mexico [M.S. thesis]: Albuquerque, University of New Mexico, 210 p.

Lambert, P. W., 1966, Notes on the late Cenozoic geology of the Taos–Questa area, New Mexico: in Northrop, S.A., and Read, C.B., eds., Taos-Raton-Spanish Peaks Country (New Mexico and Colorado): New Mexico Geological Society, 17th Annual Field Conference, Guidebook, p. 43–50.

Leininger, R. L., 1982, Cenozoic evolution of the southernmost Taos plateau, New Mexico [M.S. thesis]: Austin, University of Texas, 110 p.

Lipman, P.W., and Mehnert, H.H., 1979, The Taos plateau volcanic field, northern Rio Grande rift, New Mexico: in Riecker, R.C., ed., Rio Grande Rift: Tectonics and Magmatism: Washington, D.C., American Geophysical Union, p. 289–311.

Long, P.E., 1976, Precambrian granitic rocks of the Dixon–Peñasco area, northern New Mexico—A study in contrasts: New Mexico Bureau of Geology and Mineral Resources Open-File Report 71, 533 p.

Miller, J.P., Montgomery, A., and Sutherland, P.K., 1963, Geology of part of the southern Sangre de Cristo Mountains, New Mexico: New Mexico Bureau of Geology and Mineral Resources Memoir 11, 106 p.

Nielsen, K.C., 1972, Structural evolution of the Picuris Mountains, New Mexico [M.S. thesis]: Chapel Hill, University of North Carolina, 47 p.

Pazzaglia, F.J., 1989, Tectonic and climatic influences on the evolution of Quaternary landforms along a segmented range-front fault, Sangre de Cristo Mountains, north-central New Mexico [M.S. thesis], Albuquerque, University New Mexico, 246 p.

Rehder, T.R., 1986, Stratigraphy, sedimentology, and petrography of the Picuris Formation in Ranchos de Taos and Tres Ritos quadrangles, north-central New Mexico [M.S. thesis]: Dallas, Southern Methodist University, 110 p.

Steinpress, M.G., 1980, Neogene stratigraphy and structure of the Dixon area, Española Basin, north-central New Mexico [M.S. thesis]: Albuquerque, University of New Mexico, 127 p.

Thompson, R.A., and Machette, M.N., 1989, Geologic map of the San Luis Hills area, Conejos and Costilla counties, Colorado: U.S. Geological Survey Miscellaneous Investigations Series Map I-1906, scale 1:50,000.

# APPENDIX 2
## Inventory of wells used on geologic map and cross sections.

| Site ID | UTM easting NAD83 | UTM northing NAD83 | Elevation (ft asl) | NMOSE well record | Well depth (ft bls) |
|---|---|---|---|---|---|
| **TV-100** | 439079 | 4017493 | 7751 | RG-83352 | 1000 |
| **TV-103** | 439575 | 4020899 | 7086 | RG-88886 | 1000 |
| **TV-104** | 440789 | 4019142 | 7440 | RG-52607-CLW | 1080 |
| **TV-105** | 443044 | 4023239 | 6930 | none | 320 |
| **TV-106** | 440432 | 4019553 | 7352 | RG-27921 | 972 |
| **TV-107** | 440249 | 4019644 | 7313 | RG-37157 | 955 |
| **TV-111** | 444522 | 4023739 | 6943 | RG-50511 | 125 |
| **TV-115** | 438728 | 4022238 | 6883 | RG-55576 | 600 |
| **TV-116** | 443986 | 4024762 | 6898 | RG-90552 | 260 |
| **TV-118** | 443951 | 4023035 | 6978 | RG-18848 | 175 |
| **TV-119** | 442022 | 4024782 | 6852 | RG-64885 | 150 |
| **TV-121** | 439043 | 4024718 | 6732 | RG-67154 | 215 |
| **TV-124** | 439301 | 4024674 | 6749 | RG-83204 | 215 |
| **TV-125** | 445310 | 4020203 | 7214 | RG-82804 | 280 |
| **TV-127** | 445193 | 4020308 | 7205 | RG-45679 | 400 |
| **TV-128** | 445068 | 4020094 | 7242 | RG-57268 | 500 |
| **TV-133** | 445160 | 4019970 | 7252 | RG-81518 | 383 |
| **TV-134** | 445208 | 4019938 | 7248 | RG-83373 | 294 |
| **TV-137** | 444018 | 4026841 | 6781 | none | |
| **TV-139** | 438605 | 4022824 | 6840 | RG-88461 | 400 |
| **TV-140** | 437092 | 4021843 | 6845 | RG-76925 | 260 |
| **TV-142** | 445074 | 4024612 | 6886 | RG-35148 | 65 |
| **TV-143** | 439606 | 4025327 | 6726 | RG-83661 | 300 |
| **TV-145** | 444459 | 4027975 | 6763 | RG-41884 | 80 |
| **TV-146** | 444153 | 4025875 | 6806 | RG-85313 | 60 |
| **TV-147** | 443682 | 4027403 | 6739 | none | |
| **TV-148** | 444389 | 4025434 | 6812 | RG-91630 | 100 |
| **TV-149** | 437854 | 4022511 | 6843 | RG-77935 | 575 |
| **TV-150** | 445312 | 4028085 | 6806 | RG-78943 | 84 |
| **TV-153** | 443983 | 4024152 | 6933 | RG-75582 | 245 |
| **TV-154** | 442635 | 4026829 | 6760 | RG-49046 | 40 |
| **TV-155** | 440968 | 4026311 | 6749 | RG-39866 | 120 |
| **TV-160** | 445094 | 4022051 | 7036 | none | 125 |
| **TV-163** | 443478 | 4027212 | 6731 | none | 80 |
| **TV-165** | 440217 | 4025434 | 6732 | RG-69193 | 120 |
| **TV-166** | 438483 | 4022941 | 6823 | RG-79997 | 300 |
| **TV-167** | 442917 | 4022252 | 7000 | RG-87080 | 460 |
| **TV-168** | 443597 | 4027664 | 6759 | RG-30133 | 50 |
| **TV-171** | 440344 | 4026206 | 6667 | RG-37303-S | 3180 |
| **TV-173** | 439230 | 4024897 | 6732 | RG-83207 | 200 |
| **TV-174** | 440398 | 4026308 | 6661 | none | 144 |
| **TV-177** | 440735 | 4025672 | 6753 | none | 93 |
| **TV-182** | 444981 | 4022809 | 7008 | RG-03894-S | 244 |
| **TV-183** | 444800 | 4022144 | 7057 | RG-03894 | 185 |
| **TV-186** | 440972 | 4023357 | 6901 | RG-80614 | 280 |
| **TV-191** | 439911 | 4020631 | 7146 | RG-91446 | 1002 |
| **TV-192** | 440787 | 4023808 | 6841 | RG-50140 | 240 |
| **TV-195** | 436504 | 4023133 | 6699 | RG-87837 | 480 |
| **TV-196** | 436925 | 4023507 | 6693 | RG-80207 | 450 |
| **TV-198** | 436937 | 4023381 | 6687 | RG-80117 | 480 |
| **TV-199** | 437863 | 4024095 | 6698 | RG-87207 | 400 |
| **TV-201** | 445909 | 4020976 | 7134 | RG-62881 | 260 |
| **TV-205** | 444949 | 4020549 | 7182 | none | 60 |
| **TV-207** | 446075 | 4020810 | 7178 | RG-75724 | 598 |
| **TV-208** | 440458 | 4025995 | 6688 | none | 78 |
| **TV-209** | 444721 | 4017534 | 7500 | RG-83482 | 295 |
| **TV-211** | 444378 | 4015730 | 7840 | RG-85777 | 673 |
| **TV-212** | 444670 | 4012658 | 8365 | RG-85776 | 420 |
| **TV-213** | 443824 | 4011868 | 8492 | RG-85775 | |
| **TV-214** | 444063 | 4012668 | 8531 | RG-85772 | 580 |
| **TV-215** | 443658 | 4012416 | 8666 | RG-85771 | 420 |
| **TV-216** | 444087 | 4013519 | 8120 | RG-85773 | 420 |

| Site ID | UTM easting NAD83 | UTM northing NAD83 | Elevation (ft asl) | NMOSE well record | Well depth (ft bls) |
|---|---|---|---|---|---|
| **TV-217** | 442074 | 4022809 | 6959 | RG-73095a | 2003 |
| **TV-218** | 442074 | 4022809 | 6959 | RG-73095b | 460 |
| **TV-219** | 442093 | 4022868 | 6948 | RG-72824 | 1400 |
| **TV-220** | 444376 | 4015734 | 7840 | none | 210 |
| **TV-221** | 444372 | 4015730 | 7840 | none | 31 |
| **TV-227** | 439398 | 4025086 | 6719 | RG-83209 | 185 |
| **TV-229** | 439009 | 4020576 | 7103 | RG-63879 | 1070 |
| **TV-230** | 439362 | 4016255 | 8151 | RG-76468 | 1400 |
| **TV-232** | 441479 | 4025438 | 6806 | RG-39071 | 120 |
| **TV-233** | 440656 | 4023366 | 6888 | RG-83497 | 347 |
| **TV-234** | 445805 | 4020855 | 7139 | RG-62881POD2 | 760 |
| **TV-235** | 445894 | 4021455 | 7023 | RG-62881POD3 | 220 |
| **TV-238** | 441602 | 4026232 | 6751 | RG-67648 | 105 |
| **TV-257** | 442495 | 4023234 | 6915 | RG-82811 | 280 |
| **TV-260** | 440935 | 4024629 | 6844 | RG-80824 | 275 |
| **TV-262** | 442983 | 4024240 | 6897 | none | 200 |
| **TV-263** | 438479 | 4022658 | 6857 | RG-81875 | 700 |
| **TV-264** | 445853 | 4022032 | 6969 | RG-59636 | 210 |
| **TV-269** | 446417 | 4020675 | 7150 | RG-51208 | 109 |
| **TV-270** | 446556 | 4020963 | 7058 | RG-68552 | 420 |
| **TV-272** | 446180 | 4026771 | 6869 | RG-74545 | 2109 |
| **TV-273** | 446201 | 4026744 | 6871 | RG-74545 | 291 |
| **TV-274** | 446187 | 4026767 | 6870 | RG-74545 | 1480 |
| **TV-275** | 446208 | 4026746 | 6870 | RG-74545 | 2020 |
| **TV-276** | 444199 | 4027480 | 6753 | RG-82913 | 290 |
| **TV-280** | 443366 | 4027305 | 6726 | RG-74971 | 140 |
| **TV-282** | 446396 | 4028865 | 6846 | RG-82234 | 85 |
| **TV-283** | 445305 | 4028253 | 6804 | RG-52846 | 112 |
| **TV-288** | 440231 | 4020074 | 7257 | RG-91449 | 1005 |
| **TV-289** | 440066 | 4020322 | 7217 | RG-91454 | 1000 |
| **TV-290** | 444358 | 4028143 | 6775 | none | 1400 |

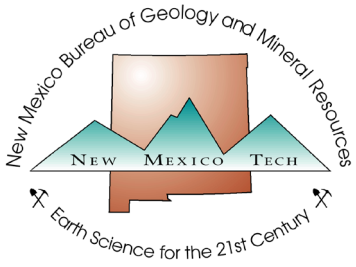


New Mexico Bureau of Geology and Mineral Resources

A division of New Mexico Institute of Mining and Technology

Socorro, NM 87801
(575) 835 5490
Fax (575) 835 6333
geoinfo.nmt.edu